

Spring 5-31-2014

## Optimizing alginate-chitosan microcapsules using co-axial air flow method as 3d stem cell microenvironment

Noel Alfonso  
*New Jersey Institute of Technology*

Follow this and additional works at: <https://digitalcommons.njit.edu/theses>



Part of the [Biomedical Engineering and Bioengineering Commons](#)

---

### Recommended Citation

Alfonso, Noel, "Optimizing alginate-chitosan microcapsules using co-axial air flow method as 3d stem cell microenvironment" (2014). *Theses*. 196.  
<https://digitalcommons.njit.edu/theses/196>

This Thesis is brought to you for free and open access by the Electronic Theses and Dissertations at Digital Commons @ NJIT. It has been accepted for inclusion in Theses by an authorized administrator of Digital Commons @ NJIT. For more information, please contact [digitalcommons@njit.edu](mailto:digitalcommons@njit.edu).

## **Copyright Warning & Restrictions**

The copyright law of the United States (Title 17, United States Code) governs the making of photocopies or other reproductions of copyrighted material.

Under certain conditions specified in the law, libraries and archives are authorized to furnish a photocopy or other reproduction. One of these specified conditions is that the photocopy or reproduction is not to be “used for any purpose other than private study, scholarship, or research.” If a user makes a request for, or later uses, a photocopy or reproduction for purposes in excess of “fair use” that user may be liable for copyright infringement,

This institution reserves the right to refuse to accept a copying order if, in its judgment, fulfillment of the order would involve violation of copyright law.

**Please Note: The author retains the copyright while the New Jersey Institute of Technology reserves the right to distribute this thesis or dissertation**

Printing note: If you do not wish to print this page, then select “Pages from: first page # to: last page #” on the print dialog screen

The Van Houten library has removed some of the personal information and all signatures from the approval page and biographical sketches of theses and dissertations in order to protect the identity of NJIT graduates and faculty.

## **ABSTRACT**

### **OPTIMIZING ALGINATE-CHITOSAN MICROCAPSULES USING CO-AXIAL AIR FLOW METHOD AS 3D STEM CELL MICROENVIRONMENT**

**by  
Noel Alfonso**

Microencapsulation of cells is gaining popular interest in the field of biomedical engineering because it provides a more effective 3D scaffold that can mimic the cell microenvironment. The benefits of using microcapsules are biocompatibility, biodegradability, nontoxicity, and formation under mild gelation conditions. In this study, the ability of the alginate microcapsules to control the proliferation and differentiation of mouse OCT4-GFP embryonic stem cells is investigated. Microcapsules are produced by extrusion of alginate into a calcium chloride gelation bath with the aid of a co-axial air flow. It is shown that the size of the spheres is controlled based on needle gauge, air flow rate, and alginate concentration. Coating the microcapsules with a chitosan membrane improves stability over time as their swelling behavior is examined. The surface of the microcapsules is further characterized using Fourier transform infrared (FTIR) spectroscopy and scanning electron microscopy (SEM). Permeability of the microcapsules is studied through the release rate of encapsulated bovine serum albumin (BSA) and fluorescein isothiocyanate-dextran (FITC-dextran) over time. Finally, cell viability is tested by means of live-dead cell and resazurin assays of encapsulated cells. The proliferation and differentiation of encapsulated mouse OCT4-GFP embryonic stem cells are analyzed by flow cytometry. It is shown that encapsulated cells are able to remain viable and that the microcapsule microenvironment is able to control the proliferation and differentiation of mouse OCT4-GFP embryonic stem cells.

**OPTIMIZING ALGINATE-CHITOSAN MICROCAPSULES USING CO-AXIAL  
AIR FLOW METHOD AS 3D STEM CELL MICROENVIRONMENT**

**by  
Noel Alfonso**

**A Thesis  
Submitted to the Faculty of  
New Jersey Institute of Technology  
in Partial Fulfillment of the Requirements for the Degree of  
Master of Science in Biomedical Engineering**

**Department of Biomedical Engineering**

**May 2014**

Blank Page

**APPROVAL PAGE**

**OPTIMIZING ALGINATE-CHITOSAN MICROCAPSULES USING CO-AXIAL  
AIR FLOW METHOD AS 3D STEM CELL MICROENVIRONMENT**

**Noel Alfonso**

---

Dr. Cheul H. Cho, Thesis Advisor Date  
Assistant Professor of Biomedical Engineering, NJIT

---

Dr. Bryan J. Pfister, Committee Member Date  
Associate Professor of Biomedical Engineering, NJIT

---

Dr. George Collins, Committee Member Date  
Research Professor of Biomedical Engineering, NJIT

## **BIOGRAPHICAL SKETCH**

**Author:** Noel Alfonso

**Degree:** Master of Science

**Date:** May 2014

### **Undergraduate and Graduate Education:**

- Master of Science in Biomedical Engineering,  
New Jersey Institute of Technology, Newark, NJ, 2014
- Bachelor of Science in Biomedical Engineering,  
New Jersey Institute of Technology, Newark, NJ, 2011

**Major:** Biomedical Engineering

*I would like to dedicate this thesis  
to my beloved parents*

## ACKNOWLEDGMENT

I would like to express my great appreciation and gratitude to my thesis advisor, Dr. Cheul H. Cho. Your patience, guidance, and knowledge were key factors necessary to complete my research. Thank you for always believing in me and encouraging me not to give up in times when I did want to just give up. You have provided me with an excellent and unforgettable experience. Another thank you goes to Dr. Bryan J. Pfister and Dr. George Collins for agreeing to be a part of my thesis committee. Their additional suggestions and feedback contributed to the success of my project. Special thanks to all of my family and friends for their continuing love and strong support. To my mother and father, Rosalinda and Noe Alfonso, thank you for always believing in me and providing me with everything to continue and complete my education. You are amazing people working very hard just to try to give their children the best lives they can live. I know it is hard trying to financially support three children through college. However, you both never seem to doubt or give up on any one of us. For that reason, I can't express the amount of unconditional love I have for you both and how much you mean to me. Finally, I wish to thank all of the members, past and present, of Dr. Cheul H. Cho's lab for their help, especially Derek Yip. Thank you for teaching me how to properly use most of the lab equipment, showing me how to culture cells, and answering the numerous questions I had regarding lab equipment, experiments, and any other problems that I came across. You are truly patient and very helpful. I could have not asked for a better colleague to work with.

## TABLE OF CONTENTS

Chapter	Page
1 INTRODUCTION .....	1
1.1 Microencapsulation Technology .....	1
1.2 Cell Choice .....	2
1.3 Methods for Microcapsule Fabrication .....	3
1.4 Microcapsule Critical Properties .....	4
1.5 Biomaterials for Microencapsulation .....	5
1.6 Objective .....	9
2 MATERIALS AND METHODS .....	10
2.1 Materials .....	10
2.2 Preparation of Encapsulation Solutions .....	11
2.3 Preparation of Alginate Microcapsules .....	11
2.4 Optimization of Alginate Microcapsule Size .....	12
2.5 Swelling and Stability Test .....	13
2.6 Sphere Surface Characterization .....	13
2.6.1 FTIR .....	14
2.6.2 Microcapsule Staining with Coomassie Protein Assay Reagent .....	14
2.6.3 Scanning Electron Microscopy .....	15
2.7 Membrane Permeability .....	15
2.7.1 BSA Encapsulation and Sustained Release .....	15
2.7.2 FITC-dextran Encapsulation and Fluorescence Intensity .....	17

**TABLE OF CONTENTS**  
**(Continued)**

<b>Chapter</b>	<b>Page</b>
2.8 Cell Studies .....	17
2.8.1 Fibroblast Cell Encapsulation for Live-dead Cell Assay .....	18
2.8.2 Fibroblast Cell Encapsulation for Resazurin Assay .....	18
2.8.3 Mouse Embryonic Stem Cell Encapsulation .....	19
3 RESULTS .....	21
3.1 Effect of Needle Gauge Size and Air Flow Rate on Alginate Microcapsule Size	21
3.2 Effect of Chitosan Coating on Microcapsule Stability .....	22
3.3 Characterization by FTIR and SEM .....	26
3.4 Permeability of Microcapsules .....	30
3.5 Microencapsulation of Cells .....	34
4 DISCUSSION .....	39
5 CONCLUSION .....	51
APPENDIX EFFECT OF ALGINATE CONCENTRATION ON MICROCAPSULE SIZE .....	52
REFERENCES .....	53

## LIST OF TABLES

<b>Table</b>	<b>Page</b>
3.1 Shape Factor Analysis of Alginate Microcapsules of Various Needle Gauges and Air Flow Rates .....	22
3.2 Shape Factor of Uncoated and Chitosan-coated Alginate Microcapsules .....	26

## LIST OF FIGURES

<b>Figure</b>	<b>Page</b>
1.1 Chemical structure of alginate monomeric units and their arrangement .....	6
1.2 Egg-box model of alginate gelation .....	7
1.3 Chemical structure of chitosan .....	8
2.1 Illustration of alginate microcapsule fabrication .....	12
3.1 Microcapsule size as determined by needle gauge and air flow rate .....	21
3.2 Swelling of uncoated and chitosan-coated alginate microcapsules .....	23
3.3 Microscopic images of swelled alginate microcapsules.....	25
3.4 FTIR readings of alginate and chitosan powders .....	27
3.5 FITR readings of uncoated and chitosan-coated alginate microcapsules .....	27
3.6 Alginate microcapsules stained with coomassie brilliant blue R-250 .....	29
3.7 SEM images of uncoated and chitosan-coated alginate microcapsules .....	30
3.8 Accumulated amount of BSA released from microcapsules .....	31
3.9 Microscopic images of encapsulated FITC-dextran over time .....	32
3.10 Measurement of average fluorescence intensity in the microcapsules .....	33
3.11 Live-dead cell analysis for encapsulated fibroblast cells .....	35
3.12 Resazurin assay result for the viability of fibroblast cells in microcapsules .....	36
3.13 Microscopic images of encapsulated mouse OCT4-GFP embryonic stem cells ...	37
3.14 Flow cytometry analysis of encapsulated mouse embryonic stem cells .....	38
4.1 Microcapsules fabricated at 20 SCFH air flow rate .....	41
4.2 Coomassie brilliant blue R-250 chemical structure .....	44

4.3	Microscopic image of mouse OCT4-GFP embryonic stem cells subculture .....	49
-----	---	----

## LIST OF SYMBOLS

ECM	Natural Extracellular Matrix
CaCl <sub>2</sub>	Calcium Chloride
PLL	Poly-L-lysine
°C	Degrees Celsius
%	Percent
FITC	Fluorescein Isothiocyanate
kDa	kilodalton
BSA	Bovine Serum Albumin
DMEM	Dulbecco's Modified Eagle Medium
M	Molar
dH <sub>2</sub> O	Deionized Water
mL	Milliliter
cm	Centimeter
rpm	Revolutions Per Minute
SCFH	Standard Cubic Feet per Hour
PBS	Phosphate Buffer Saline
FTIR	Fourier Transform Infrared
SEM	Scanning Electron Microscopy
mg	Milligram

HEPES	4-(2-Hydroxyethyl) piperazine-1-ethanesulfonic acid
$\mu\text{g}$	Microgram
nm	Nanometer
$\mu\text{L}$	Microliter
NaCl	Sodium Chloride
mM	Millimolar
PFA	Paraformaldehyde
FACS	Fluorescence-activated Cell Sorting
mm	Millimeter
FBS	Fetal Bovine Serum

# CHAPTER 1

## INTRODUCTION

### 1.1 Microencapsulation Technology

Cell therapy is becoming one of the popular methods to replace, repair, or enhance the function of damaged tissues or organs. Prior to use, cells are maintained and cultured in vitro until it has reached its desired therapeutic state. The traditional methods of manipulating cells in a two dimensional (2D) culture system, such as Petri dishes, T-flasks, or multi-wells surfaces, are becoming insufficient for the need of modern medicine. These culturing conditions have limitations in not providing the necessary surface area needed for cell growth. Consequently, the cells are unable to grow and expand in a large scale, which is required in cell therapeutic applications. Another method of using cells for therapy involves the injection of cells at the site of injury or defect. In regenerative medicine, the injection of cells at a defect site may be problematic as cells can not directly adhere to the tissue and could be washed away into the surrounding environment. The problems of 2D culture systems and cell lost at implantation site are the reasons why injectable transporter materials, such as microcapsules, are gaining interest as cell carriers for tissue engineering [1]. The microencapsulation of cells is proven to be a valuable model in the research of gene therapy, artificial cells and organs, large-scale cell culture, and drug screening [4]. Cell microencapsulation involves the packaging of cells within a semi-permeable membrane. This membrane allows for the bi-directional diffusion of nutrients, oxygen, secreted therapeutic products, and metabolic wastes. It also prevents the diffusion of high molecular weight substances, such as antibodies and immunocytes, from the cells [4].

Microcapsules are also able to protect the encapsulated cells from the harsh external environment and immune response of the host and thus maintaining its useful biological activity. The encapsulation of cells can also eliminate or reduce the use of immunosuppressant drugs if an immune response is triggered.

In addition, microcapsules transition the two dimensional (2D) culture systems into three dimensional (3D). This 3D culture system provides a special microenvironment that can affect the encapsulated cellular behaviors. Microcapsules are able to provide a 3D matrix that better mimic the geometry, chemistry, and signaling environment of the natural extra cellular matrix (ECM) of cells in vivo. Therefore, the use of microcapsules can better control the encapsulated cell properties.

## **1.2 Cell Choice**

The choice of cell type for encapsulation depends on the intended application of the microcapsules. Various cell types such as primary cells, stem cells, and bioengineered cells have been considered potentially therapeutic for the treatment of many diseases [6]. A potential problem associated with the encapsulation of nonautologous cells is the high immunogenicity of the encapsulated cells which can trigger an unwanted immune response in the microenvironment surrounding the microcapsule. This can lead to the suffocation and death of the encapsulated cells. Additionally, differentiated cells are limited in availability. One possible solution to overcome these problems is to choose a cell type that can reduce the host immune response and that are readily available. Stem cells are becoming a popular cell choice for microencapsulation technology.

Stem cells are a popular cell choice in regenerative medicine because they have the capability of reconstituting damaged tissues and maintaining normal tissues. They

are also a good choice for tissues that do not have the ability to regenerate. Briefly, stem cells are undifferentiated cells that have the ability to self-renew and differentiate. The two major classes of stem cells are embryonic stem (ES) cells and adult stem cells. Adult stem cells are known to be tissue specific. This means that the microenvironment in which it came from determines the specific lineages the cell is able to differentiate into. On the other hand, embryonic stem cells have the potential of becoming more than one type of cell and are termed to be pluripotent. In either case, the differentiation of stem cells depends on the microenvironment in which it resides.

### **1.3 Methods for Microcapsule Fabrication**

Various fabrication methods exist for the production of microcapsules. Some of these techniques include spray-drying, vibrating nozzle, air-blast or twin-fluid atomization, emulsification or gelation, jet-cutting, extrusion under an electrostatic field, layer-by-layer self assembly, and milling and grinding [1, 5]. The details of each method will not be discussed. Although each process has its advantages, it also has some disadvantages. Each technique contains parameters that may be detrimental to the encapsulating material. For example, the spray-drying technique is regarded as harsh because the drying gas requires a high temperature at which is harmful to sensitive biological materials. The vibrating nozzle and jet-cutting methods are only limited to small-scale production. In air-blast or twin-fluid atomization, the process is complicated and the extrusion solution is subjected to both tensile and shear stresses. Emulsification or gelation requires many steps and rigid control of both the temperature and viscosity of emulsion. In addition, the microcapsules must be washed thoroughly to remove the residual oil or organic solvents. The application of an electrostatic field with a high

voltage is known to be a limitation for the extrusion under an electrostatic field method. The fabrication process for layer-by-layer self assembly is quite complicated. Milling and grinding method requires large amounts of material, and this technique may result in the denaturation of proteins due to the high pressure at the pushing and grinding inlets. The mechanical stress may cause degradation of the proteins [5]. The choice of technique depends on the desired properties and application under study. In particular, a gentle encapsulation technique is required if the viability of encapsulated cells is aimed. The fabrication method chosen for this study involves the extrusion of the microcapsule solution through a syringe needle with an air flow jet applied at the needle tip. This method is effective, very simply, and relatively cheap.

#### **1.4 Microcapsule Critical Properties**

Some of the favorable properties of microcapsules include mild gelation conditions, biocompatibility, biodegradability, and nontoxicity [2]. Biocompatibility is defined as the ability of a biomaterial to perform with an appropriate host response in a specific application [6]. Furthermore, the microcapsule must not trigger an immune response if implantation into a host is intended. For cell encapsulation, the microcapsule must have sufficient permeability to allow the nutrients and oxygen to enter and the metabolic cellular wastes products to leave the capsule in order to maintain cell viability and promote cell growth [1, 4]. In addition, the pores must be small enough such that unwanted large molecules will not enter or leave the capsule [1]. The microcapsules must also be able to maintain long term stability and integrity. In cell encapsulation, the membrane isolates the cells from the external microenvironment of the host. It must provide a strong barrier to ensure that there is no direct cell-cell contact between the

encapsulated cells and the host cells that can lead to an unwanted immune response. The size of the microcapsules is also carefully considered as it found that it can influence the immune response on the microcapsules as well [6]. Sakai et al. concluded that the cellular reaction was much lower with the use of smaller microcapsules when compared to microcapsules of larger diameters [7]. This study tries to achieve these requirements necessary for the maintenance of cell function, growth, and viability of encapsulated cells.

### **1.5 Biomaterials for Microencapsulation**

Biomaterials, such as polysaccharide-based hydrogels, are becoming increasingly important in the development of drug delivery systems and tissue engineering approaches[6]. Natural polymers are typically chosen as the primary components for microencapsulation due to their biocompatibility and biodegradability [8]. Most microcapsules that have been developed are alginate-based with a liquid core in the center. Some of the advantages of using alginate include low toxicity and high biocompatibility with the host and with enclosed cells [3]. Alginates are natural polysaccharides derived from brown algae whose structure consists of two monomeric units,  $\alpha$ -L-guluronic (G) and  $\beta$ -D-mannuronic (M) acid residues, that are linked by 1-4 glycoside bonds [3, 8, 9]. These residues are arranged linearly in homopolymeric blocks (GG and MM) and in heteropolymeric blocks (GM) [9]. Figure 1.1 shows the structure of the two monomeric units of alginate and their arrangement. Alginates are highly hydrophilic due to the presence of  $-\text{OH}$  and  $-\text{COOH}$  groups in its chains.

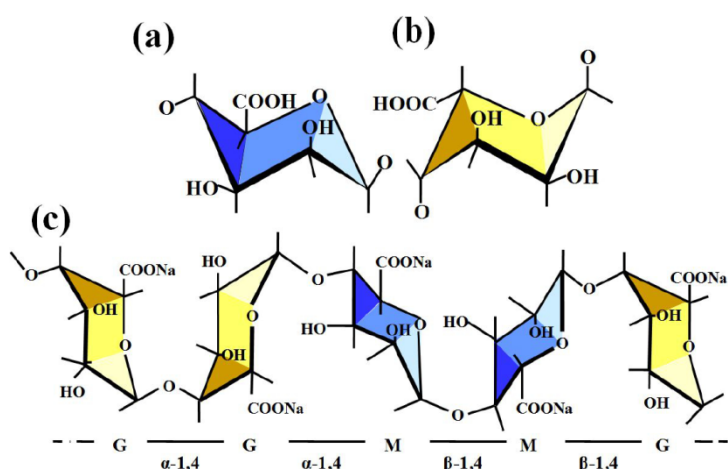


**Figure 1.1** Alginate is composed of two monomeric units, (a) β-D-mannuronic acid and (b) α-L-guluronic acid. These two units are arranged linearly as shown in (c).

Source: Keita Kashima and Masanao Imai (2012). *Advanced Membrane Material from Marine Biological Polymer and Sensitive Molecular-Size Recognition for Promising Separation Technology*, Advancing Desalination, Prof. Robert Y. Ning (Ed.), ISBN: 978-953-51-0704-0, InTech, DOI: 10.5772/50734. Available from: <http://www.intechopen.com/books/advancing-desalination/advanced-membrane-material-from-marine-biological-polymer-and-sensitive-molecular-size-recognition-f>

Alginates are also known to form gels under relatively mild conditions at room temperature which allows the preservation of the biological activity of the encapsulated material [8]. The simplest and widely used method for the production of alginate microcapsules is based on the dropwise extrusion of alginate solution through a syringe with a needle into a gelation bath containing divalent cations. The gelation of alginate polymers is formed through cross-linking between the carboxylate anions of guluronic acid and divalent cations [2, 8, 9]. This phenomenon is referred to as the egg-box model in which a divalent cation binds to two carboxyl groups on the adjacent alginate molecules [9]. The egg-box model is illustrated in Figure 1.2. The result is a highly compacted gel network. The selection of the divalent cations is carefully considered. For example, monovalent cations and magnesium ions ( $Mg^{2+}$ ) do not induce gelation with

alginate. On the other hand, other divalent cations such as lead ( $\text{Pb}^{2+}$ ), copper ( $\text{Cu}^{2+}$ ), cadmium ( $\text{Cd}^{2+}$ ), cobalt ( $\text{Co}^{2+}$ ), nickel ( $\text{Ni}^{2+}$ ), zinc ( $\text{Zn}^{2+}$ ), and manganese ( $\text{Mn}^{2+}$ ) is able to induce gelation. However, they are not used because they are known to be toxic. The commonly used divalent cation for the gelation of alginate is calcium ( $\text{Ca}^{2+}$ ) in calcium chloride ( $\text{CaCl}_2$ ) due to its biocompatibility and nontoxicity.

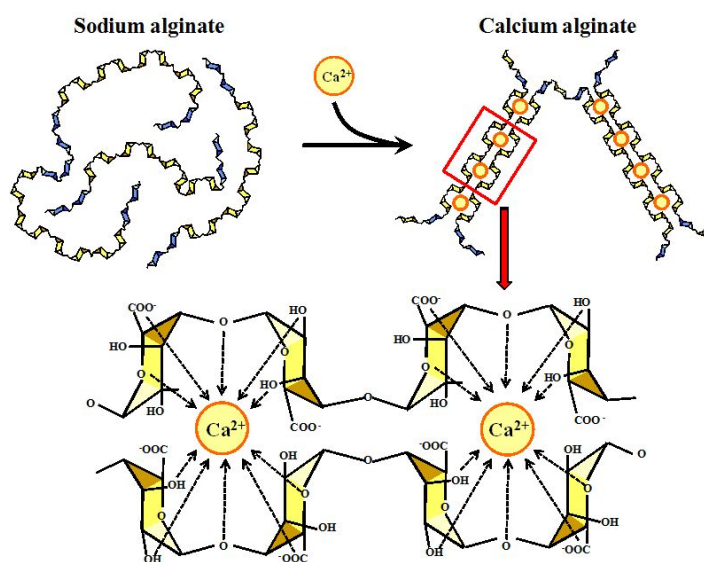


**Figure 1.2** The gelation of the alginate polymer is formed when a divalent cation binds to the alginate.

Source: Keita Kashima and Masanao Imai (2012). Advanced Membrane Material from Marine Biological Polymer and Sensitive Molecular-Size Recognition for Promising Separation Technology, Advancing Desalination, Prof. Robert Y. Ning (Ed.), ISBN: 978-953-51-0704-0, InTech, DOI: 10.5772/50734. Available from: <http://www.intechopen.com/books/advancing-desalination/advanced-membrane-material-from-marine-biological-polymer-and-sensitive-molecular-size-recognition-f>

The long term structural integrity of the alginate gel network is questioned given the soft gelatinous nature of the material [10]. Since the gelation of alginate involves the ionic interaction between negatively charged alginate molecules and positively charged divalent cations, it may be possible for the divalent cations to diffuse out of the alginate matrix over a prolonged period. This would cause the bond between alginate and the

divalent cation to weaken resulting in a weaker gel that may dissolve or break [10]. Coating of the microcapsules with a polycation, such as poly-L-lysine (PLL) or chitosan, can help stabilize the ionic gel network and reduce alginate permeability through electrostatic interactions with the negatively charged alginate acid groups [2, 8]. Chitosan is gaining interest in replacing PLL in coating alginate microcapsules [11]. PLL is reported to induce foreign body reactions by activating macrophages and fibroblasts [11]. Chitosan is a naturally occurring polycationic polymer derived from the natural polymer chitin, which is found in the exoskeleton of crustaceans and insects [2]. Chitosan is also a polysaccharide with structural characteristics similar to glycosaminoglycans [11]. The structure of chitosan is given in Figure 1.3.

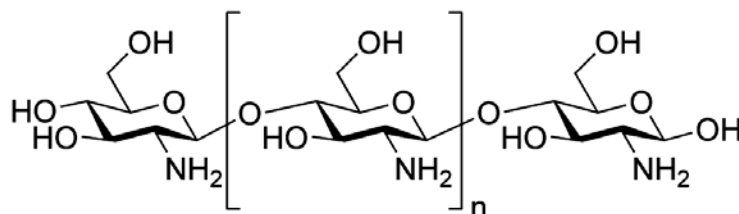


**Figure 1.3** The structure of chitosan is comprised of D-glucosamine and N-acetylglucosamine with unique polycation characteristics.

Source: Thayza Christina Montenegro Stamford, Thatiana Montenegro Stamford-Arnaud, Horacina Maria de Medeiros Cavalcante, Rui Oliveira Macedo and Galba Maria de Campos-Takaki (2013). Microbiological Chitosan: Potential Application as Anticariogenic Agent, Practical Applications in Biomedical Engineering, Dr. Adriano Andrade (Ed.), ISBN: 978-953-51-0924-2, InTech, DOI: 10.5772/54453. Available from: <http://www.intechopen.com/books/practical-applications-in-biomedical-engineering/microbiological-chitosan-potential-application-as-anticariogenic-agent>

Chitosan is freely available and relatively cheap compared to PLL. Furthermore, it is known to be nontoxic and bioabsorbable. It has been investigated as a suitable polymer coating for oral delivery of proteins as well as the immobilization or delivery of living cells. Chitosan is soluble in acid solutions when the pH is less than 6.0. Thus,

acetic acid is often commonly used for preparing chitosan solutions for encapsulation processes. Due to their excellent compatibility and nontoxicity, this study utilizes alginate as the microcapsule material and chitosan as the coating material.

### **1.6 Objective**

The goal of this study is to optimize alginate-based microcapsules using a co-axial air flow method and apply these microcapsules as a 3D stem cell microenvironment. Specifically, the aims are (1) to fabricate and characterize alginate and alginate-chitosan microcapsules using a co-axial air flow method and (2) to evaluate cell encapsulation on cytocompatibility and stem cell proliferation and differentiation. In this project, it is hypothesized that the alginate-based 3D microenvironment is able to control the proliferation and differentiation of embryonic stem cells.

## **CHAPTER 2**

### **MATERIALS AND METHODS**

#### **2.1 Materials**

Alginic acid sodium salt from brown algae (250 cps at 25°C, 2% solution), low molecular weight chitosan (20 cps), coomassie brilliant blue R-250, and fluorescein isothiocyanate-dextran (FITC-dextran, molecular weight of 70kDa) are purchased from Sigma-Aldrich, USA. Anhydrous calcium chloride, sodium chloride, sodium citrate, bovine serum albumin (BSA, bp 600-100), ethanol (95% denatured with MIKB), sodium cacodylate (Na-cacodylate) buffer, and glutaraldehyde (25% solution) are obtained from Fisher Scientific, USA. Glacial acetic acid is provided by Ricca Chemical Company, USA.

Fibroblast cells are cultured and maintained in fibroblast cell medium consisting of 1% penicillin-streptomycin, 10% horse serum, and 89% Dulbecco's Modified Eagle Medium (DMEM) high glucose. The fibroblast cells are passaged every one to two weeks. The medium in the tissue culture dish is replaced every three days until time of passage. Fibroblast cells are incubated at culture conditions of 37°C and 10% CO<sub>2</sub>.

Mouse OCT4-GFP embryonic stem cells are cultured and maintained in undifferentiation medium consisting of ESGRO Murine Leukemic Inhibitory Factor (10<sup>6</sup> units)(Millipore), 0.1mM 2-mercaptoethanol, 1.5M sodium bicarbonate, nonessential amino acids, 4mM L-glutamine, penicillin-streptomycin, knockout serum replacement, and knockout DMEM. The mouse OCT4-GFP embryonic stem cells are passaged every two to three days with medium change occurring every day. Mouse OCT4-GFP embryonic stem cells are incubated at culture conditions of 37°C and 10% CO<sub>2</sub>.

## 2.2 Preparation of Encapsulation Solutions

Sodium alginate powder and calcium chloride pellets are weighed and dissolved in deionized water (dH<sub>2</sub>O) separately. Low molecular weight chitosan powder is weighed and added to 0.15M CaCl<sub>2</sub> solution making a chitosan solution of concentration 0.4%. Next, 0.5% glacial acetic acid is added. This solution is placed on a stirring plate and mixed overnight at room temperature to ensure dissolving. The solution is then filtered using a cell strainer to remove any debris and impurities from the solution. The solution is kept at 4°C until it is time to be used.

## 2.3 Preparation of Alginate Microcapsules

Sodium alginate is dissolved in deionized water (dH<sub>2</sub>O). The alginate microcapsules are generally formed by extruding 1mL of alginate solution through a syringe with a needle gauge into a gelling bath containing 20mL of 0.15M calcium chloride (CaCl<sub>2</sub>) dissolved in dH<sub>2</sub>O. The distance from the tip of the syringe needle and the CaCl<sub>2</sub> gelation bath is about 5cm. An air flow by means of an air flowmeter is applied to the bottom end of the syringe as the alginate solution is extruded. After extrusion, the alginate microcapsules are incubated in the 0.15M CaCl<sub>2</sub> solution for 5-10 minutes at a stirring rate of about 60 revolutions per minute (rpm). This fabrication method is illustrated in Figure 2.1.

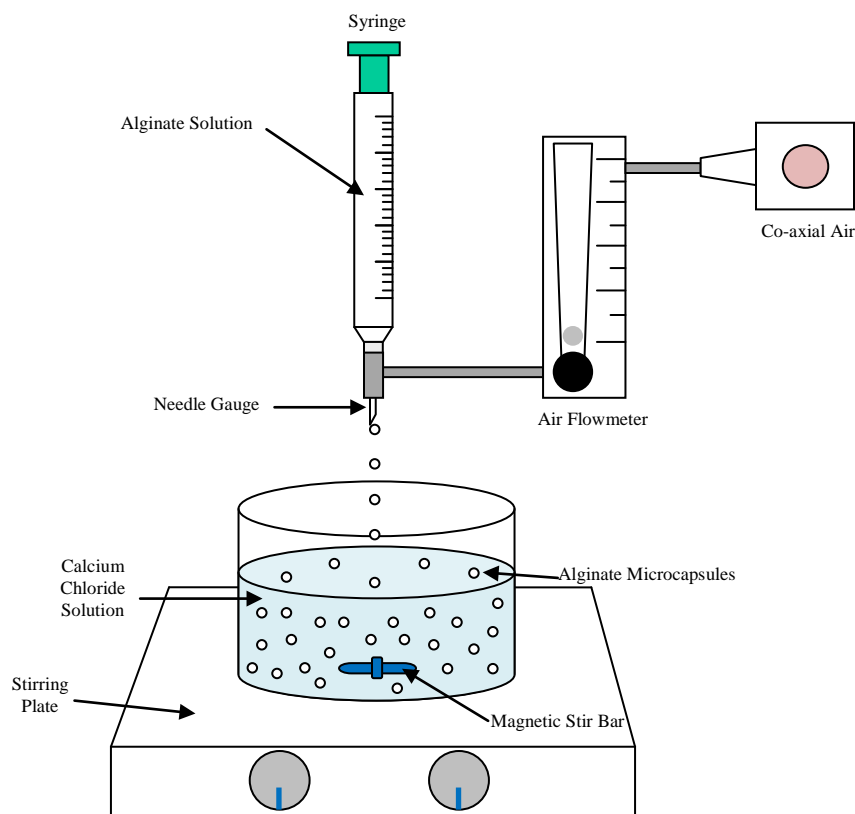


**Figure 2.1** The fabrication process of alginate microcapsules involves extruding the alginate solution into a calcium chloride gelation bath under gentle stirring. An air flow is applied at the end of the syringe needle to aid in the microsphere formation.

#### 2.4 Optimization of Alginate Microcapsule Size

The size of alginate microcapsules can be controlled based on adjusting certain variables. Initially in this study, the effect of needle gauge size and air flow rate are investigated. An alginate concentration of 1.5% is used and the method of fabrication is described in Section 2.3. Alginate microcapsules are prepared using both 22 and 30 gauge needles. For each needle gauge, an air flow rate is applied at the needle as the alginate solution is extruded into the  $\text{CaCl}_2$  solution under gentle stirring. Air flow rates of 0 SCFH, 7.5 SCFH, 10 SCFH, 15 SCFH, and 20 SCFH are tested. After extrusion and incubation in 0.15M  $\text{CaCl}_2$  solution, the microcapsules are transferred into p60 non-treated tissue

culture dishes and observed under an inverted light microscope at 2x magnification. Images are acquired via a Nikon digital camera connected to the microscope. The microcapsules' area, mean diameter, and shape factor are measured using SigmaScan Pro 5 software.

### **2.5 Swelling and Stability Test**

The effect of coating the alginate microcapsules with a chitosan membrane is studied. The swelling and stability of chitosan-coated microcapsules over time are compared with uncoated alginate microcapsules. Microcapsules are produced as described in Section 2.3. Briefly, an alginate concentration of 1.5% is extruded through a syringe with a 30 gauge needle into a 0.15M CaCl<sub>2</sub> solution under gentle stirring. An air flow rate of 15 SCFH is applied at the end of the syringe. Incubating the capsules in 0.4% chitosan in 0.15M CaCl<sub>2</sub> solution for 10 minutes following incubation in CaCl<sub>2</sub> proceeding extrusion completion creates chitosan-coated microcapsules. Both uncoated and chitosan-coated alginate microcapsules are washed with dH<sub>2</sub>O and incubated in phosphate buffer saline (PBS) at room temperature. Microcapsules are observed under an inverted light microscope at 2x magnification until rupture is evident. Images are taken with a Nikon digital camera connected to the microscope. The microcapsules' area, mean diameter, and shape factor are measured using SigmaScan Pro 5 software.

### **2.6 Sphere Surface Characterization**

The surface comparison of uncoated and chitosan-coated alginate microcapsules is examined. FTIR characterization is used to detect the presence and absence of chitosan on the coated and uncoated alginate microcapsules, respectively. In addition,

microcapsules are stained with 5x coomassie brilliant blue R-250 and compared to discover success of coating with chitosan. Scanning electron microscopy evaluates the difference in topography between the two microcapsule conditions.

### **2.6.1 FITR**

Alginate microcapsules, both coated and chitosan-coated, are fabricated according to the aforementioned methods in Sections 2.3 and 2.5. Following the incubation in  $\text{CaCl}_2$  for the uncoated alginate microcapsules and the incubation in 0.4% chitosan in 0.15M  $\text{CaCl}_2$  for the chitosan-coated alginate microcapsules, the microcapsules are transferred into p35 non-treated tissue culture dishes. Excess solutions are removed and the microcapsules are washed with  $\text{dH}_2\text{O}$ . The  $\text{dH}_2\text{O}$  is then aspirated and the microcapsules are placed into a vacuum desiccator to dry for at least 24 hours. After 24 hours, the microcapsules are analyzed using Spectrum 100 FTIR Spectrometer (Perkin Elmer).

### **2.6.2 Microcapsule Staining with Coomassie Protein Assay Reagent**

The method of manufacturing uncoated and chitosan-coated alginate microcapsules is similar to the technique described in Sections 2.3 and 2.5. Following fabrication, the microcapsules are washed with  $\text{dH}_2\text{O}$  and incubated in 5x coomassie brilliant blue R-250 for about 10 minutes. After 10 minutes, the coomassie brilliant blue R-250 is aspirated. The microcapsules are washed with  $\text{dH}_2\text{O}$  and incubated in  $\text{dH}_2\text{O}$ . Microcapsules are observed under an inverted light microscope at 4x magnification. Images are taken with a Nikon digital camera connected to the microscope.

### **2.6.3 Scanning Electron Microscopy**

Uncoated and chitosan-coated alginate microcapsules are produced following the same protocol performed in Sections 2.3 and 2.5. After the incubation in  $\text{CaCl}_2$  for the uncoated alginate microcapsules and the incubation in 0.4% chitosan in 0.15M  $\text{CaCl}_2$  for the chitosan-coated alginate microcapsules, the microcapsules are incubated in 2.5% glutaraldehyde in 0.1M Na-cacodylate buffer (pH = 7.4) overnight at 4°C. Next, the solution is aspirated and the microcapsules are washed with 0.1M Na-cacodylate buffer two times. Microcapsules are dehydrated through the incubation in a series of ethanol for 5-10 minutes each. The series are 30%, 50%, 70%, and 95% ethanol. After the aspiration of 95% ethanol, the microcapsules are placed in a chemical hood to air dry. Prior to scanning the samples, the microcapsules are mounted on metal stubs using double-sided adhesive tape, and coated with gold under a vacuum using a sputter coater unit. The samples are then examined by scanning electron microscopy (SEM) (LEO 1350 VP).

## **2.7 Membrane Permeability**

The membrane permeability of both uncoated and chitosan-coated alginate microcapsules is studied through the encapsulation of BSA and FITC-dextran. The release rate of each is monitored over time and quantified.

### **2.7.1 BSA Encapsulation and Sustained Release**

To prepare the BSA encapsulated microcapsule, BSA is first dissolved in  $\text{dH}_2\text{O}$  resulting in a BSA stock solution concentration of 400mg/mL. The BSA stock solution is then mixed with 2.5% alginate solution resulting in a final BSA concentration of 20mg/mL.

The BSA-alginate solution is extruded dropwise into 20mL of 0.15M CaCl<sub>2</sub> under gentle stirring through a syringe with a 30 gauge needle. An air flow rate of 15 SCFH is applied at the needle gauge to aid in microcapsule formation. The microcapsules are incubated in the CaCl<sub>2</sub> at a stirring rate of 60 rpm for about 10 minutes. The microcapsules are transferred and evenly distributed into three 3mL test tubes. Any excess CaCl<sub>2</sub> in the test tubes is aspirated. The microcapsules are incubated in HEPES buffer solution and the test tube is placed into a water bath at 37°C for incubation. At time points 10, 15, 75 minutes, and days 1, 2, 3, 4, 5, 6, 7 after extrusion completion, a 1mL sample of incubation solution is taken. The remaining solution is aspirated and replaced with 2mL of fresh HEPES buffer solution. The Bradford colorimetric protein assay is used to detect the amount of protein secreted from uncoated and chitosan-coated alginate microcapsules containing BSA. Ten BSA standards are prepared using a two-fold serial dilution beginning with BSA stock solution concentration of 500µg/mL. The incubation solution samples and the ten BSA standards are placed into a 96-well plate and mixed with Coomassie brilliant blue R-250. The samples and standards are analyzed by a spectrophotometer at a wavelength of 650nm using the software SoftMax Pro.

The effect of coating the microcapsules with chitosan on the release rate of encapsulated BSA is also tested. To create microcapsules with a chitosan coating, the microcapsules are transferred into 0.4% chitosan solution in 0.15M CaCl<sub>2</sub> after 10 minutes of incubation in CaCl<sub>2</sub> under gentle stirring. The microcapsules are incubated in the chitosan solution for 5 minutes. After 5 minutes, the same protocol for the uncoated microcapsules is followed starting from the transfer of the microcapsules into a 3mL test tube.

### **2.7.2 FITC-dextran Encapsulation and Fluorescence Intensity**

FITC-dextran encapsulated microcapsules are prepared by mixing 50mg/mL stock solution of FITC-dextran with 2.5% alginate solution. The resulting final concentration of encapsulated FITC-dextran is 1mg/mL. The FITC-dextran-alginate solution is extruded into 20mL of 0.15 CaCl<sub>2</sub> under gentle stirring through a syringe with a 30 gauge needle. An air flow rate of 15 SCFH is applied at the needle gauge to aid in microcapsule fabrication. Upon extrusion completion, the microcapsules are incubated in the CaCl<sub>2</sub> solution at a stirring rate of 60 rpm for about 5 minutes. Next, the microcapsules are transferred into a p60 non-treated tissue culture dish. The excess CaCl<sub>2</sub> in the dish is aspirated, the microcapsules are washed with HEPES buffer solution one time, and fresh HEPES buffer is added as the incubation medium. Chitosan-coated microcapsules are created by incubating the microcapsules in 0.4% chitosan in 0.15M CaCl<sub>2</sub> for 5 minutes after incubation in CaCl<sub>2</sub> following extrusion completion. The microcapsules are observed under a fluorescence microscope for 2 days at 2x magnification. Images of the microcapsules are taken with a Nikon digital camera connected to the microscope. The microcapsules' average fluorescence intensity is measured using SigmaScan Pro 5 software.

## **2.8 Cell Studies**

The alginate microcapsule microenvironment is explored through the encapsulation of cells. The viability of encapsulated fibroblast cells are examined through live-dead cell and resazurin assays. The encapsulation of mouse OCT4-GFP embryonic stem cells is studied to determine the effect of the microcapsule environment on stem cell proliferation and differentiation.

### **2.8.1 Fibroblast Cell Encapsulation for Live-dead Cell Assay**

Encapsulated fibroblast cells in alginate microcapsules are produced by mixing about 1.5 million fibroblast cells of passage 15 with 1mL of 2.5% alginate solution. The cell-alginate solution is extruded through a syringe with a 30 gauge needle into 20mL of 0.15M CaCl<sub>2</sub> at a stirring rate of 60 rpm. An air flow rate of 15 SCFH is applied at the needle gauge. After extrusion completion, the microcapsules are incubated in the CaCl<sub>2</sub> under gentle stirring for 5 minutes. Cells encapsulated in chitosan-coated microcapsules are created by incubating the microcapsules in 0.4% chitosan in 0.15M CaCl<sub>2</sub> for an additional 5 minutes following the incubation in 0.15M CaCl<sub>2</sub> after extrusion completion. The microcapsules are then transferred into four wells of a 24-well tissue culture plate. The excess CaCl<sub>2</sub> in the wells are aspirated and the microcapsules are washed with HEPES buffer solution one time. The microcapsules are incubated in 400μL of staining solution for 5 minutes. The staining solution consists of HEPES buffer solution, calcein-AM, and ethidium homodimer-1. After 5 minutes, the microcapsules are observed using a fluorescence microscope at 2x magnification for live-dead cell analysis. Images are taken by means of a Nikon digital camera connected to the microscope.

### **2.8.2 Fibroblast Cell Encapsulation for Resazurin Assay**

The method of encapsulation of fibroblast cells is similar to that described in Section 2.8.1. After the washing of the microcapsules with HEPES buffer solution, 450μL of fibroblast medium and 50μL of 10x resazurin solution are added to each well containing fibroblast encapsulated spheres. The encapsulated fibroblast cells are incubated in this solution for at least 1 hour at 37°C and 10% CO<sub>2</sub>. After 1 hour, a 100μL of the solution is sampled from each well and placed into a 96-well plate. The remaining solution in the

wells is aspirated and 500 $\mu$ L of fresh fibroblast medium is added. The 24-well plate containing the microcapsules is incubated at 37°C and 10% CO<sub>2</sub>. The collected samples are analyzed using a spectrofluorometer (Gemini XPS Fluorescence Microplate Reader) that would measure the fluorescence. The samples are measured at an excitation wavelength of 530nm and an emission wavelength of 590nm. The incubation and sampling of the resazurin solution is repeated for 5 days.

### **2.8.3 Mouse Embryonic Stem Cell Encapsulation**

About 2 million mouse OCT4-GFP embryonic stem cells of passage 41 are encapsulated in alginate microcapsules following the same fabrication method described in Section 2.8.1 for the encapsulation of fibroblast cells. The microcapsules are transferred into p60 treated tissue culture dishes. The excess CaCl<sub>2</sub> in the dish is aspirated and 4mL of differentiation medium is added. The differentiation medium consists of DMEM, 10% fetal bovine serum (FBS), 1% penicillin-streptomycin, and 4mM L-glutamine. The cells in the alginate microcapsules are maintained in culture in differentiation medium at culture conditions of 37°C and 10% CO<sub>2</sub> for 2 days with medium change occurring every day.

After 2 days of culture, the differentiation medium is aspirated and the microcapsules are washed with PBS. In order to release the cells, the microcapsules are incubated in 0.2% NaCl in 100mM sodium citrate solution at 37°C for 30 minutes. The cells in solution are collected into a 15mL conical tube and PBS is added. The tube is then centrifuged at 800rpm for 5 minutes. Following centrifuge, the supernatant is discarded. Next, the cells are incubated in 1mL of 1.6% paraformaldehyde (PFA) for 20 minutes at room temperature. After 20 minutes, about 9mL of PBS is added. The

mixture is centrifuged and the cells are resuspended in PBS. As a control condition, about 1 million undifferentiated OCT4-GFP mouse embryonic stem cells of passage 42 are fixed with 1.6% paraformaldehyde following the same procedure just described. The cells are characterized using flow cytometry by means of fluorescence-activated cell sorting (FACS).

## CHAPTER 3

### RESULTS

#### 3.1 Effect of Needle Gauge Size and Air Flow Rate on Alginate Microcapsule Size

Alginate microcapsules are fabricated by the extrusion of an alginate solution having a concentration of 1.5% through a syringe into a 0.15M CaCl<sub>2</sub> coagulation bath. Needle gauges of size 22 and 30 and the application of various air flow rates at the needle end are used to aid in the microcapsule fabrication. Following fabrication, the alginate microcapsules' area, mean diameter, and shape factor are analyzed using SigmaScan Pro 5. Shape factor measures the morphology of the microcapsules, and ranges from 0 to 1. The microcapsule can be associated to be a sphere if their shape factor value is 1 or close to 1; otherwise to an ellipse. The results are summarized in Figure 3.1 and Table 3.1.

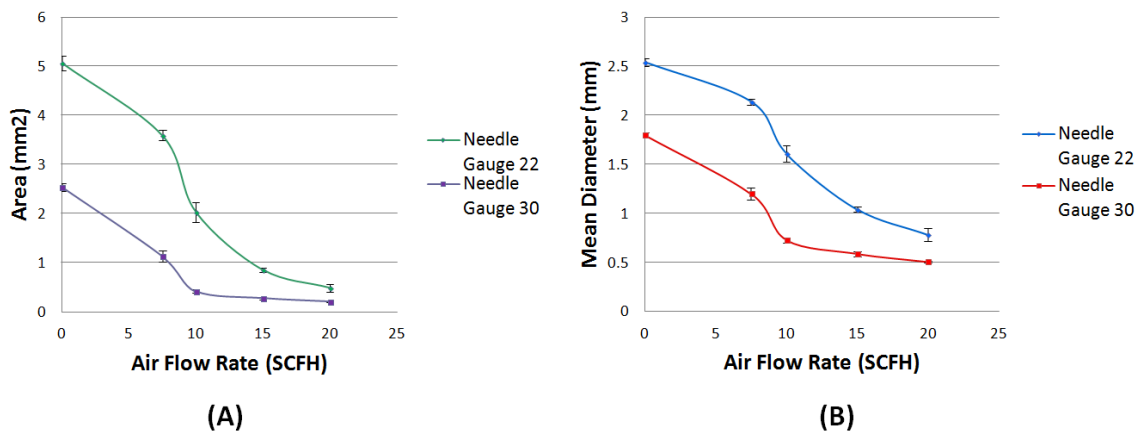


**Figure 3.1** Alginate microcapsules are fabricated with both 22 and 30 gauge needles. For each needle gauge, different air flow rates are applied at the needle tip. Both needle gauge size and air flow rate affect the size of alginate microcapsules. Comparison of microcapsule area is shown in (A) and mean diameter in (B). Data are expressed as mean  $\pm$  standard deviation.

As shown in Figure 3.1, the size of the alginate microcapsules decreases as both the needle gauge size and air flow rate increases. All the alginate microcapsules that are produced by both 22 and 30 gauge needles at the various air flow rates reveal no significant difference in morphology. Most of the alginate microcapsules produced in all conditions have shape factor values within the 0.87-0.89 range as it is given in Table 3.1. Since these values are relatively close to 1, this indicates a round morphology for the microcapsules.

**Table 3.1** Shape Factor Analysis of Alginate Microcapsule of Various Needle Gauges and Air Flow Rates

Air Flow Rate (SCFH)	Needle Gauge 22	Needle Gauge 30
0	0.872 ± 0.006	0.891 ± 0.001
7.5	0.873 ± 0.013	0.893 ± 0.001
10	0.881 ± 0.007	0.895 ± 0.002
15	0.885 ± 0.001	0.897 ± 0.002
20	0.883 ± 0.007	0.892 ± 0.003

### 3.2 Effect of Chitosan Coating on Microcapsule Stability

Adding an additional chitosan membrane on the alginate microcapsules is studied to observe the effect it has on microcapsule stability. After the fabrication of the alginate microcapsules using 1.5% alginate by extrusion through a syringe with a 30 gauge needle and an air flow rate of 15 SCFH into a CaCl<sub>2</sub> gelling bath, the microcapsules are incubated in 0.4% chitosan in 0.15M CaCl<sub>2</sub> solution for 5 minutes. Microcapsules are washed with dH<sub>2</sub>O and incubated in PBS at room temperature for a few days. The microcapsules are observed under an inverted light microscope at 2x magnification each day until microcapsule rupture. The swelling and stability of uncoated and chitosan-

coated microcapsules are compared. The microcapsules' area, mean diameter, and shape factor are analyzed using SigmaScan Pro 5. The results are represented in Figure 3.2 and Table 3.2.

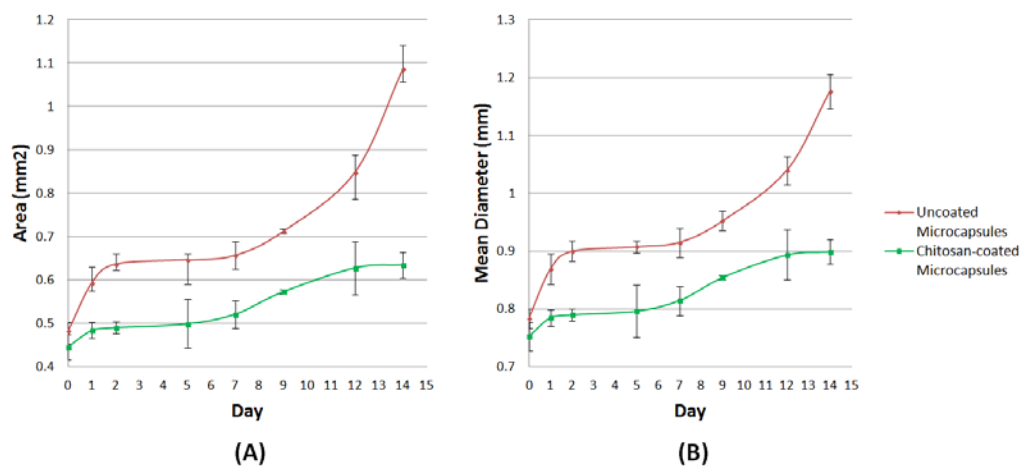


**Figure 3.2** The swelling and stability of uncoated and chitosan-coated alginate microcapsules are investigated. Microcapsules are incubated in PBS and observed under an inverted light microscope for two weeks. Comparison of microcapsule area is shown in (A) and mean diameter in (B). Data are expressed as mean  $\pm$  standard deviation.

Referring to Figure 3.2, both uncoated and chitosan-coated microcapsules produced from 1.5% alginate solution extruded through a 30 gauge needle with an air flow rate of 15 SCFH have an average mean diameter of about 0.75-0.80mm following fabrication. After the first day, all of the microcapsules show signs of swelling due to water absorption. Uncoated microcapsules show more signs of swelling as their average mean diameter increased to about 0.89mm which is a 14% increase. The average mean diameter of chitosan-coated microcapsules increased 4% from their original size to 0.78mm, which is still relatively close to the average mean diameter on the first day following fabrication. The microcapsules continue to swell as it is evident by the increase of mean diameter and area each day. After day 14, the mean diameter and area

of uncoated alginate microcapsules decrease dramatically as they indicate rupture of the microcapsules. This means that by day 14, the uncoated alginate microcapsules have reached their maximum size. By this time the average mean diameter of the uncoated alginate microcapsules is about 1.78mm, which is approximately a 1mm increase. The uncoated alginate microcapsules are swelled to more than twice their original size. On the other hand, the chitosan-coated alginate microcapsules continue to remain stable and swell. Comparing to the maximum size of uncoated microcapsules before rupture, the average mean diameter of chitosan-coated microcapsules is measured to be about 0.90mm. Their time of rupture is not known for monitoring ended on day 16 when the rupture of the uncoated alginate microcapsules was observed. The average mean diameter of the chitosan-coated microcapsules on day 16 is about 0.91mm. Figure 3.3 shows the images of the uncoated and chitosan-coated alginate microcapsules following fabrication and day 16.

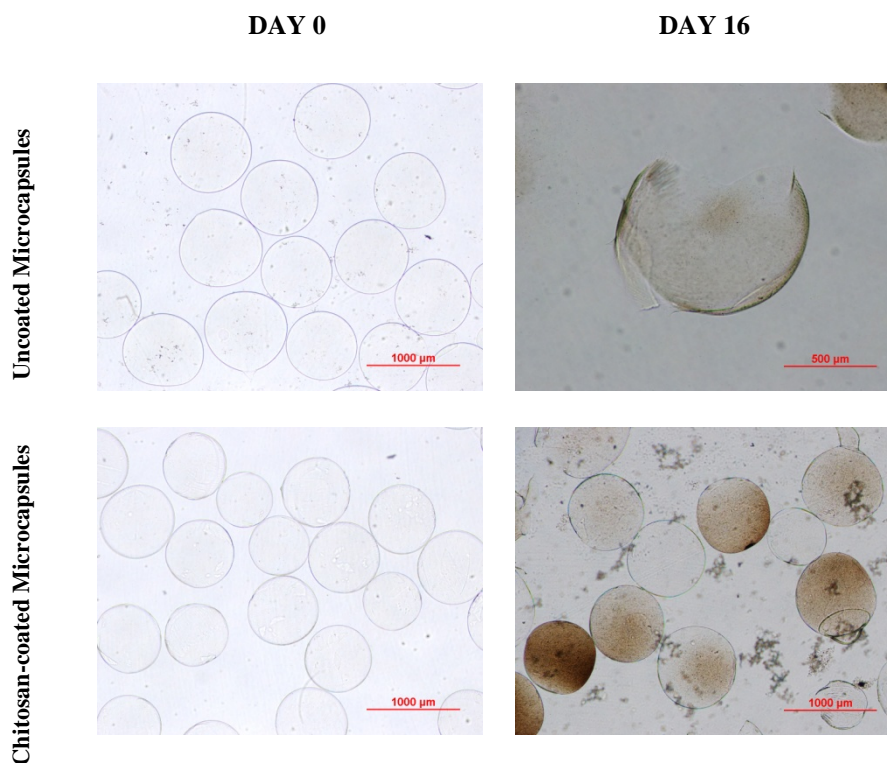


**Figure 3.3** Microscopic images of uncoated and chitosan-coated alginate microcapsules taken on day 0 following fabrication and day 16. Images are taken with a Nikon digital camera connected to an inverted light microscope. For the images of uncoated microcapsules, microcapsules are viewed at 2x magnification on day 0 and at 4x magnification on day 16. For the images of chitosan-coated microcapsules, microcapsules are viewed at 2x magnification on days 0 and 16. On day 0, microcapsules are stable and have not yet swelled. By day 16, uncoated alginate microcapsules have ruptured while chitosan-coated microcapsules remain stable.

The results illustrated in Figure 3.2 prove that coating the alginate microcapsules with a chitosan membrane offers a more stable sphere with a reduced swelling rate compared to uncoated alginate microcapsules.

Despite the increase in area and mean diameter over time, both uncoated and chitosan-coated alginate microcapsules are able to maintain their circular shape as given by their shape factor values for the 16 days of observation. All the microcapsules of both conditions have shape factor values of about 0.89 as it can be seen in Table 3.2.

**Table 3.2** Shape Factor of Uncoated and Chitosan-coated Alginate Microcapsules

Day	Uncoated	Chitosan-coated
0	0.897 ± 0.003	0.896 ± 0.002
1	0.896 ± 0.001	0.894 ± 0.005
2	0.894 ± 0.007	0.896 ± 0.003
5	0.898 ± 0.002	0.901 ± 0.002
7	0.893 ± 0.007	0.889 ± 0.007
9	0.890 ± 0.004	0.887 ± 0.014
12	0.897 ± 0.002	0.892 ± 0.006
14	0.892 ± 0.007	0.893 ± 0.006
16	0.884 ± 0.004	0.894 ± 0.003

### 3.3 Characterization of Microcapsule Surface

Uncoated and coated alginate microcapsules vary from each other based on the chemical composition on their outer surface. The surface distinction between the microcapsules is characterized using FTIR, coomassie brilliant blue R-250 staining, and SEM.

After the fabrication and drying of the uncoated and chitosan-coated alginate microcapsules, FTIR is used to determine the particular functional groups present on the surface. The microcapsule FITR spectra are compared with the FTIR readings of alginate and chitosan compounds. All samples are read at scan number 100 and a resolution at  $8\text{cm}^{-1}$ . Figures 3.4 and 3.5 provide the FTIR spectra for uncoated and chitosan-coated alginate microcapsules as well as alginate and chitosan, respectively.

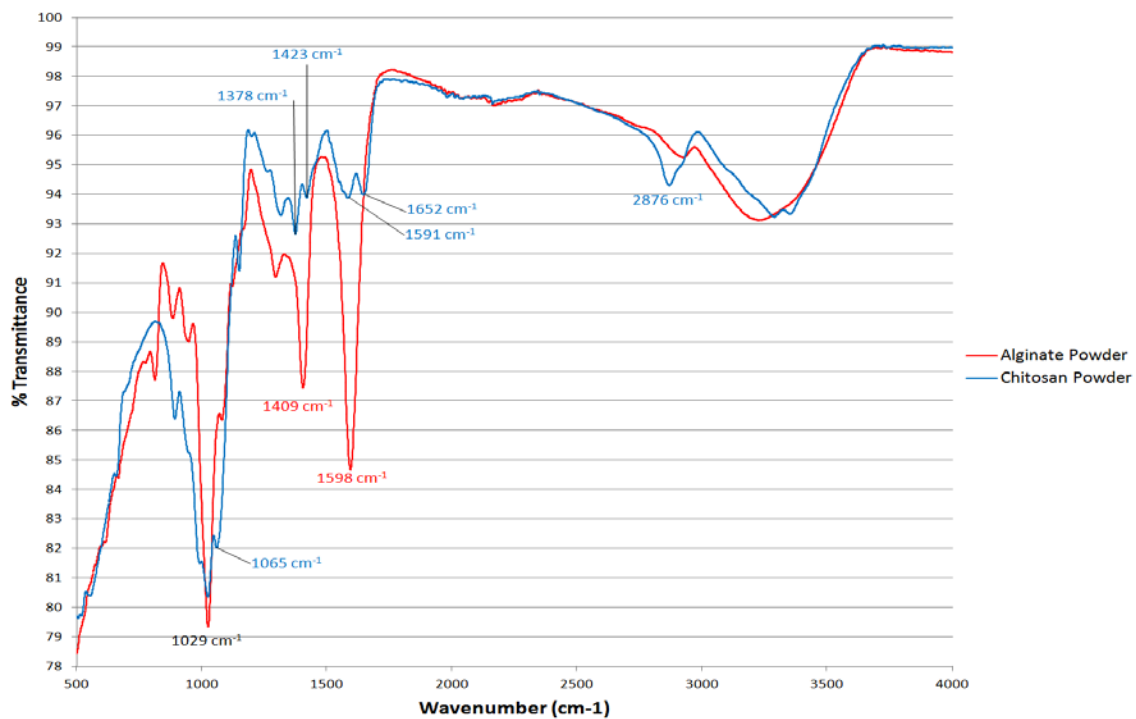


**Figure 3.4** The FTIR spectra of alginate and chitosan powders are compared with the FTIR spectra of uncoated and chitosan-coated alginate microcapsules.

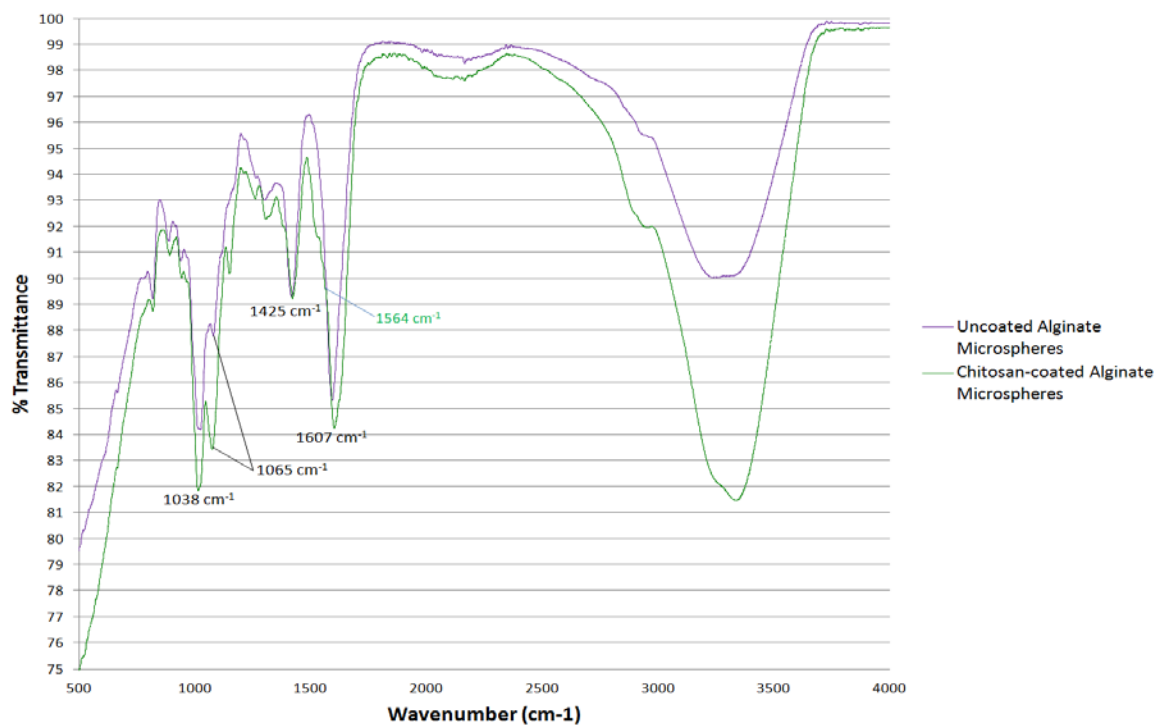


**Figure 3.5** The surface of both uncoated and chitosan-coated alginate microcapsules are characterized using FTIR.

It is important to recall the chemical structures of both alginate and chitosan presented in Figures 1.1 and 1.3, respectively, in order to associate the peaks of the FTIR spectra with the appropriate functional group. The FTIR spectrum of chitosan powder in Figure 3.4 shows a weak band of  $\text{-OH}$  stretching at  $2876\text{cm}^{-1}$ . An absorption band of the carbonyl ( $\text{C=O}$ ) stretching of the secondary amide (amide I band) is observed at  $1652\text{cm}^{-1}$ . The bending vibrations of the  $\text{N-H}$  ( $\text{N-acetylated}$  residues, amide II band) can be found at wavenumber at  $1591\text{cm}^{-1}$ . The peaks at  $1423\text{cm}^{-1}$  and  $1378\text{cm}^{-1}$  correspond to the  $\text{N-H}$  stretching of the amide and ether bonds and  $\text{N-H}$  stretching (amide III band), respectively. The peaks at  $1065\text{cm}^{-1}$  and  $1029\text{cm}^{-1}$  are the secondary (characteristic peak of  $\text{-CH-OH}$  in cyclic alcohols,  $\text{C-O}$  stretch) and primary (characteristic peak of  $\text{-CH}_2\text{-OH}$  in primary alcohols,  $\text{C-O}$  stretch) hydroxyl groups, respectively. The strong absorption peaks on the FTIR spectrum of alginate appear at  $1598\text{cm}^{-1}$  and  $1409\text{cm}^{-1}$  for the asymmetric and symmetric stretching vibrations of carboxyl anions. The bridge oxygen ( $\text{C-O-C}$ , cyclic ether) stretching bands are observed at  $1029\text{cm}^{-1}$  [12].

The plot in Figure 3.5 shows the ability of FTIR to detect the presence of chitosan on the alginate microcapsules. In both FTIR spectra of uncoated and chitosan-coated alginate microcapsules, the characteristic absorption band peaks of alginate and chitosan at  $1607\text{cm}^{-1}$ ,  $1425\text{cm}^{-1}$ ,  $1079\text{cm}^{-1}$ , and  $1038\text{cm}^{-1}$  are observed. The absorption band at  $1590\text{cm}^{-1}$  of chitosan in Figure 3.4 shifts to  $1605\text{cm}^{-1}$  after the reaction with alginate as seen in Figure 3.5. Although similar peaks are relatively obvious on both curves, there are peaks that are not so noticeable that differentiates the two curves. The important peak that is present on the chitosan-coated alginate microcapsule curve and not present on the uncoated alginate microcapsule curve occurs at wavenumber  $1564\text{cm}^{-1}$ . This peaks

indicates the presence of a  $\text{-NH}_2$  functional group in the bending position. The detection of the  $\text{-NH}_2$  functional group proves that chitosan can be detected on the surface of the coated alginate microcapsules.

Next, staining the microcapsules with 5x coomassie brilliant blue R-250 following fabrication is used to detect the presence of chitosan on the surface of the spheres. Microcapsules are observed under an inverted light microscope at 4x magnification and images are taken with a Nikon digital camera connected to a microscope. The microscopic images of the stained alginate microcapsules are illustrated in Figure 3.6.

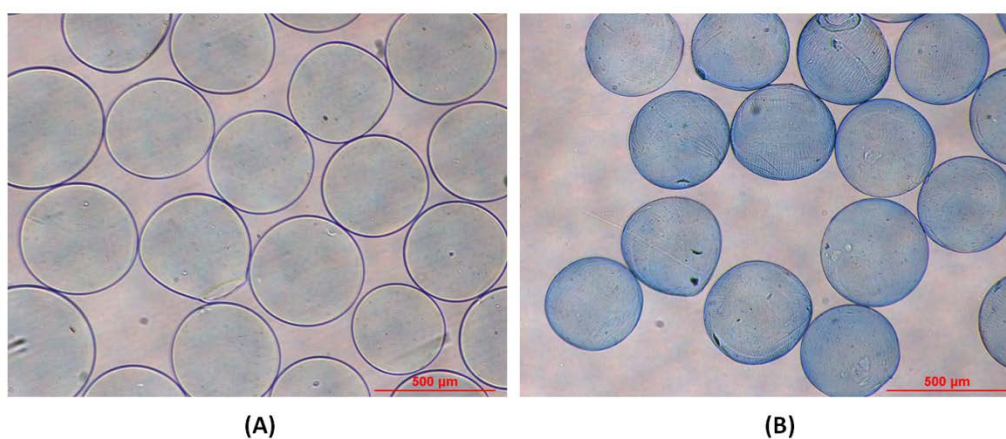


**Figure 3.6** Uncoated (A) and chitosan-coated (B) alginate microcapsules are stained with 5x coomassie brilliant blue R-250 and compared. Staining is successful in all the microcapsules. However, the coomassie brilliant blue R-250 is more evident in the chitosan-coated alginate microcapsules compared to the uncoated alginate microcapsules.

Finally, scanning electron microscopy is used to examine the difference in surface topography between uncoated and chitosan-coated alginate microcapsules. The SEM images in Figure 3.7 show the distinction between the two conditions. The SEM micrographs of dried alginate microcapsules in Figure 3.7 (A) and (C) show the surface

to be relatively smooth with a few wrinkles. The incorporation of chitosan on the microcapsule surface does not cause any significant change in the overall shape and size. However, the surface of chitosan-coated alginate microcapsules doesn't seem as smooth as the uncoated alginate microcapsules. They tend to have more wrinkles on the surface compared to the uncoated microcapsules.

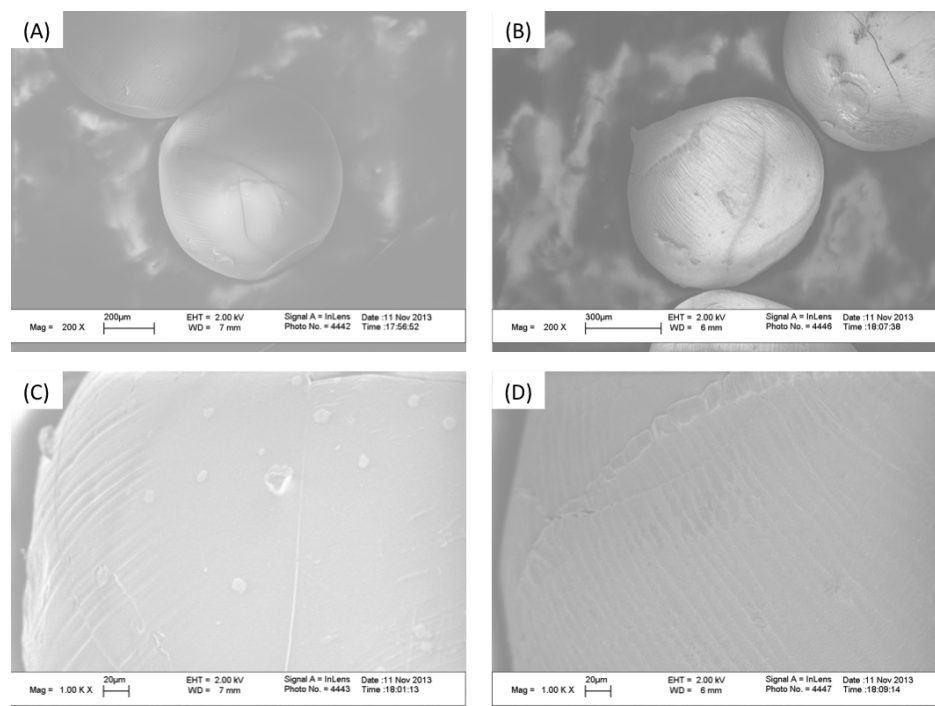


**Figure 3.7** Scanning electron microscope (SEM) images (A) and (B) show an overview at 200x magnification for uncoated and chitosan-coated microcapsules, respectively. Images (C) and (D) show the surface structure at 1Kx magnification of uncoated and chitosan-coated alginate microcapsules, respectively.

### 3.4 Permeability of Microcapsules

The permeability of the uncoated and chitosan-coated alginate microcapsules is studied through the encapsulation of BSA and FITC-dextran. Both BSA and FITC-dextran are encapsulated in the microcapsules through mixing with the alginate solution prior to

extrusion into the  $\text{CaCl}_2$  coagulation bath. The microcapsules are incubated in HEPES buffer solution over time. The release rate of each are monitored and quantified.

The permeability of BSA is analyzed through the quantification of the amount of BSA released each day. The measurement of the accumulated amount of BSA is presented in Figure 3.8. The amount of BSA released from the microcapsules during the fabrication and washing steps is shown in Figure 3.8 (A). From Figure 3.8 (A), a significant amount of BSA is released during the initial time period, particularly during the washing steps. An estimated amount of 40% of the encapsulated BSA is released from both microcapsule conditions. The amount of BSA released from the microcapsules each day proceeding fabrication is given in Figure 3.8 (B). As it is expected, BSA diffuses out of the microcapsules each day in a sustained release profile. However, more BSA is released from uncoated alginate microcapsules compared to the chitosan-coated alginate microcapsules.

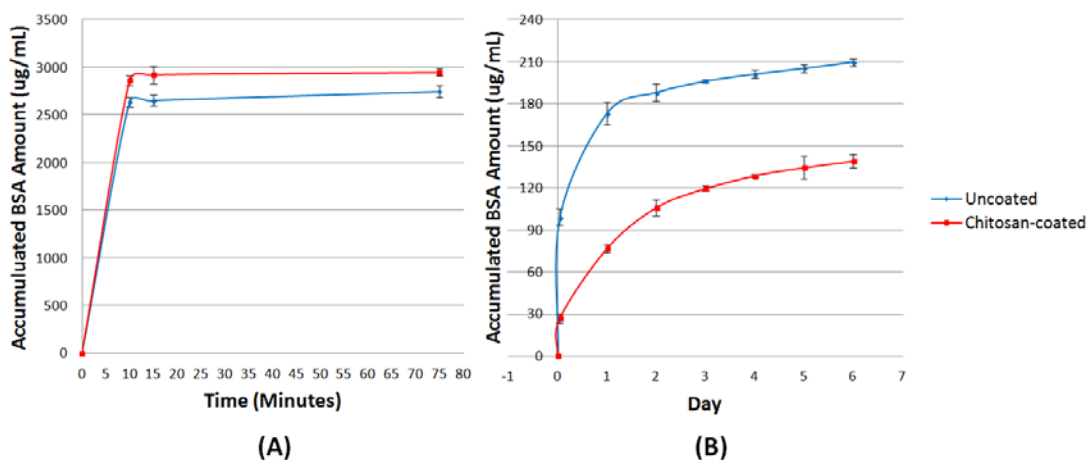


**Figure 3.8** The accumulated amount of BSA released from both uncoated and chitosan-coated alginate microcapsules is quantified by the Bradford colorimetric protein assay using a spectrophotometer. (A) illustrates the accumulated amount of BSA released from the microcapsules during the fabrication and washing steps. (B) provides the accumulated release of BSA curves for uncoated and chitosan-coated microcapsules. Data are expressed as mean  $\pm$  standard deviation.

The encapsulation of FITC-dextran is next investigated. The permeability of FITC-dextran is evaluated by measuring the fluorescence intensity in the microcapsules each day using SigmaScan Pro 5. Figure 3.9 shows the microscopic images of encapsulated FITC-dextran in uncoated and chitosan-coated alginate microcapsules on each day for 2 days.

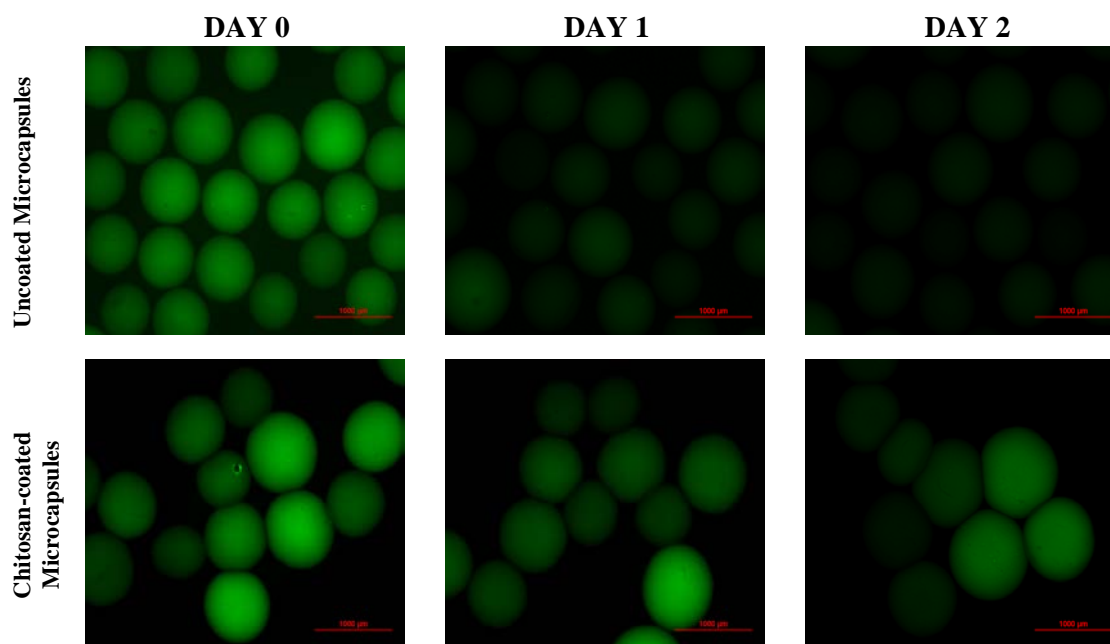


**Figure 3.9** The microphotographs of encapsulated FITC-dextran in uncoated and chitosan-coated alginate microcapsules are shown above. Images are captured with an inverted light microscope at 2x magnification.

From the microscopic images in Figure 3.9, it is evident that FITC-dextran is able to diffuse out of the microcapsules over time. After the first day of incubation in HEPES buffer solution, a significant amount of FITC-dextran is released from the uncoated alginate microcapsules compared to the chitosan-coated alginate microcapsules. By day 2, the fluorescence of the uncoated alginate microcapsules is barely noticeable when viewed under the inverted light microscope. On the other hand, the fluorescence of the

chitosan-coated alginate microcapsules is still detectable. The microcapsules are also observed on day 3, but the data are not presented here. On day 3, the fluorescence of the uncoated alginate microcapsules is not observed at all. The chitosan-coated alginate microcapsules are able to display some fluorescence, but it is barely visible. Using the microscopic images in Figure 3.9, the average fluorescence intensity of the microcapsules are measured using SigmaScan Pro 5.0 software. The results are presented in Figure 3.10.

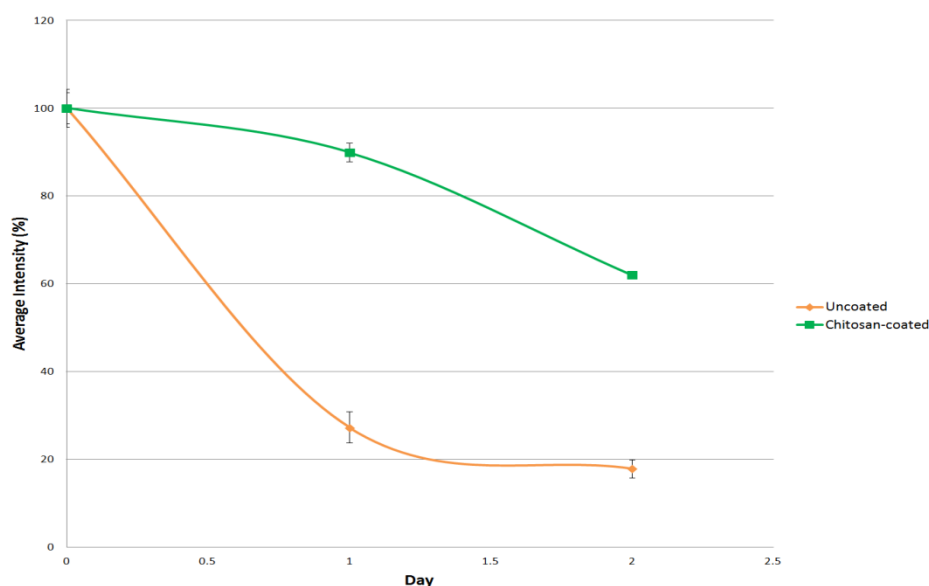


**Figure 3.10** The average fluorescence intensity of encapsulated FITC-dextran tends to decrease over time as they are released from the microcapsules. Data are expressed as mean  $\pm$  standard deviation.

The plot of average intensity in the microcapsules over time in Figure 3.10 correlates with the visual observation of the fluorescence intensity in the microcapsules in Figure 3.9. A significant amount of FITC-dextran is released after the first day of incubation in HEPES buffer solution from the uncoated alginate microcapsules; thus reducing its average fluorescence intensity from 100% down to 27%. By day 2, the

average fluorescence intensity is decreased to about 18%. FITC-dextran is slowly diffused out of the chitosan-coated alginate microcapsules as their fluorescence remain strongly evident after the first day. The average fluorescence intensity of the chitosan-coated alginate microcapsules decreases from 100% to 90%. By day 2, the average fluorescence intensity is measured to be about 62%.

The encapsulation of BSA and FITC-dextran studies reveal that the permeability of chitosan-coated alginate microcapsules is reduced compared to uncoated alginate microcapsules. This is evident through the slower release of both BSA and FITC-dextran from the chitosan-coated microcapsules. These studies also prove that the permeability of the microcapsules can be controlled by coating the alginate microcapsules with chitosan.

### **3.5 Microencapsulation of Cells**

The effect of the alginate microcapsule microenvironment on cell viability, proliferation, and differentiation is studied. The encapsulation of fibroblast cells is used to determine if cells are able to remain viable throughout the fabrication process of the microcapsules and during incubation. Cell viability is tested by means of live-dead cell and resazurin assays. The results from the live-dead cell assay are presented in Figure 3.11. The microcapsules are observed using a fluorescence microscope at 2x magnification. Microscopic images of phase, live, dead, and live-dead states are taken with a Nikon digital camera connected to the microscope. The generation of microcapsules by the co-axial air flow method did not significantly affect the viability of encapsulated fibroblast cells. As it can be seen in Figure 3.11, approximately 70% of the cells remained viable in both uncoated and chitosan-coated alginate microcapsules following the fabrication

process. The results show that fibroblasts cells can be encapsulated in alginate microcapsules while maintaining their viability.

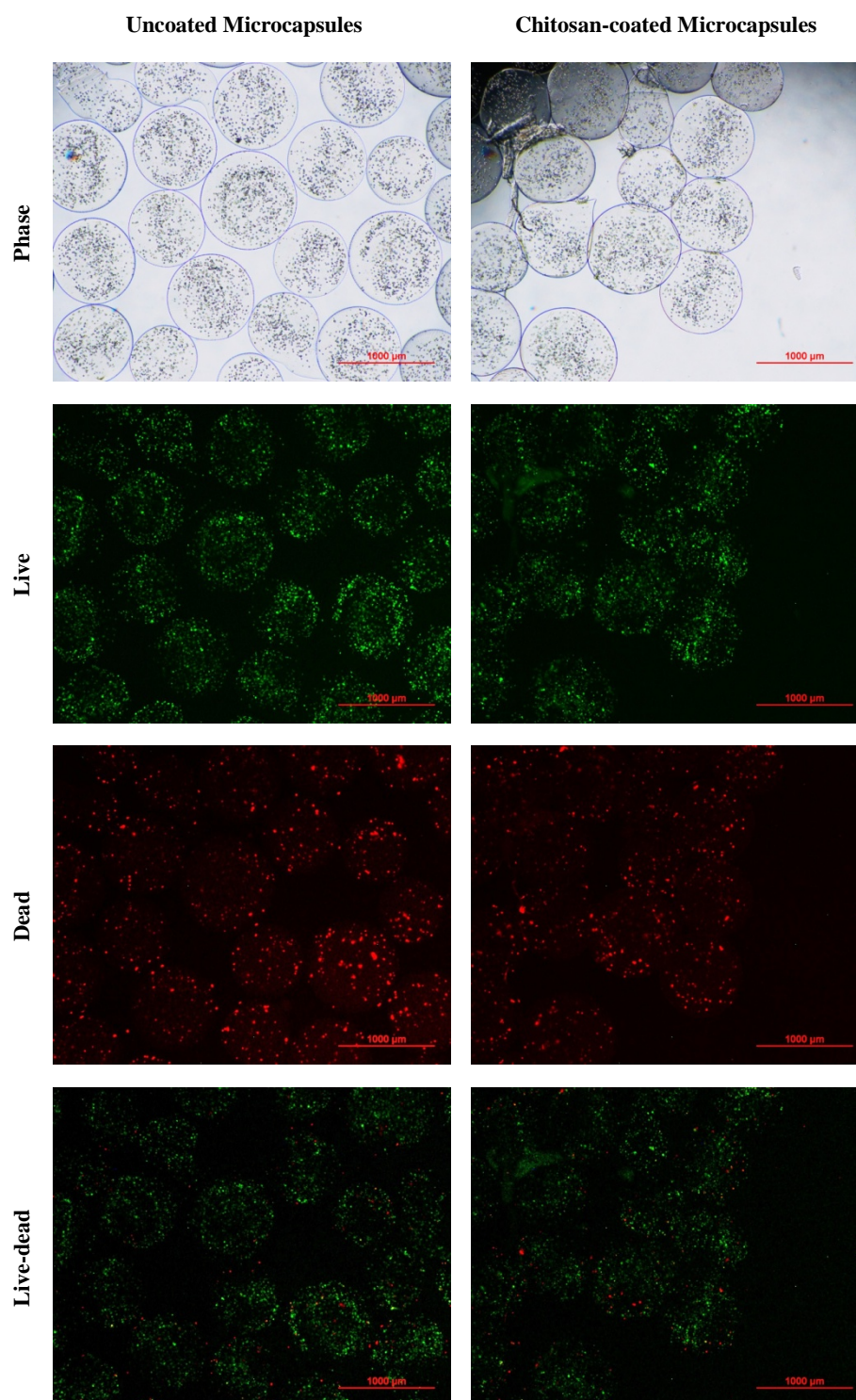


**Figure 3.11** Live-dead cell assay for fibroblast cells encapsulated in alginate microcapsules.

The resazurin assay is used to determine whether cells are able to remain alive during incubation for a couple of days. The resazurin assay quantifies the number of viable cells within the uncoated and chitosan-coated alginate microcapsules over time.

Figure 3.12 illustrates the result from the resazurin assay.

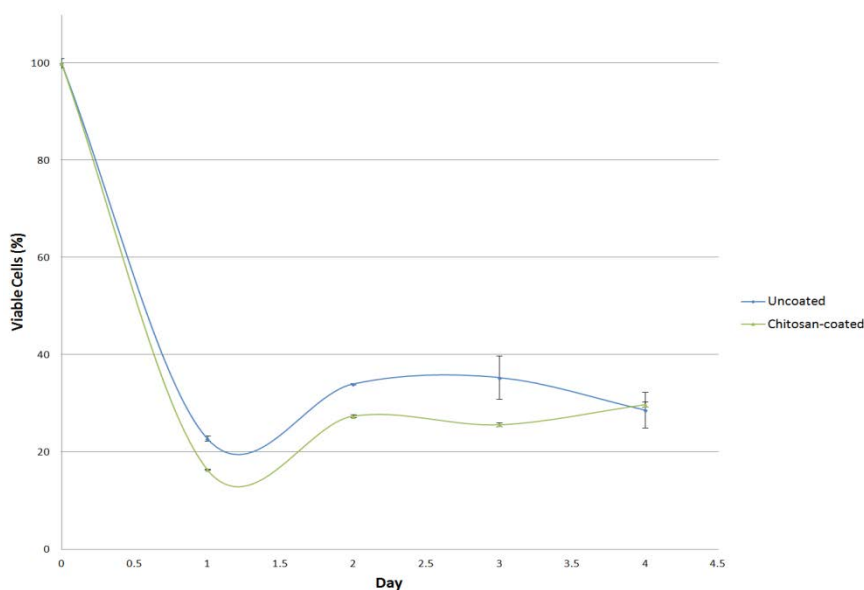


**Figure 3.12** The viability of fibroblast cells is examined through a resazurin assay. In both uncoated and chitosan-coated alginate microcapsules, the number of live cells decreased over time. Data are expressed as mean  $\pm$  standard deviation.

Based on the plot in Figure 3.12, the number of viable cells is similar in uncoated and chitosan-coated alginate microcapsules. In both cases, the number of viable fibroblast cells decreases over time during incubation. However, there appears to be more viable fibroblast cells in the uncoated alginate microcapsules compared to the chitosan-coated alginate microcapsules. After the first day, about 23% and 16% of the cells remain viable in uncoated and chitosan-coated alginate microcapsules, respectively. By day 2, there is an increase in the number of viable cells; but the number continues to decline for the following days.

The effect of the microcapsule microenvironment on the proliferation and differentiation of stem cells is also investigated. Images of encapsulated mouse OCT4-GFP embryonic stem cells in uncoated and chitosan coated alginate microcapsules as well as the GFP expression of the encapsulated cells are provided in Figure 3.13. Images are taken at 4x magnification with a Nikon digital camera connected to an inverted light microscope.

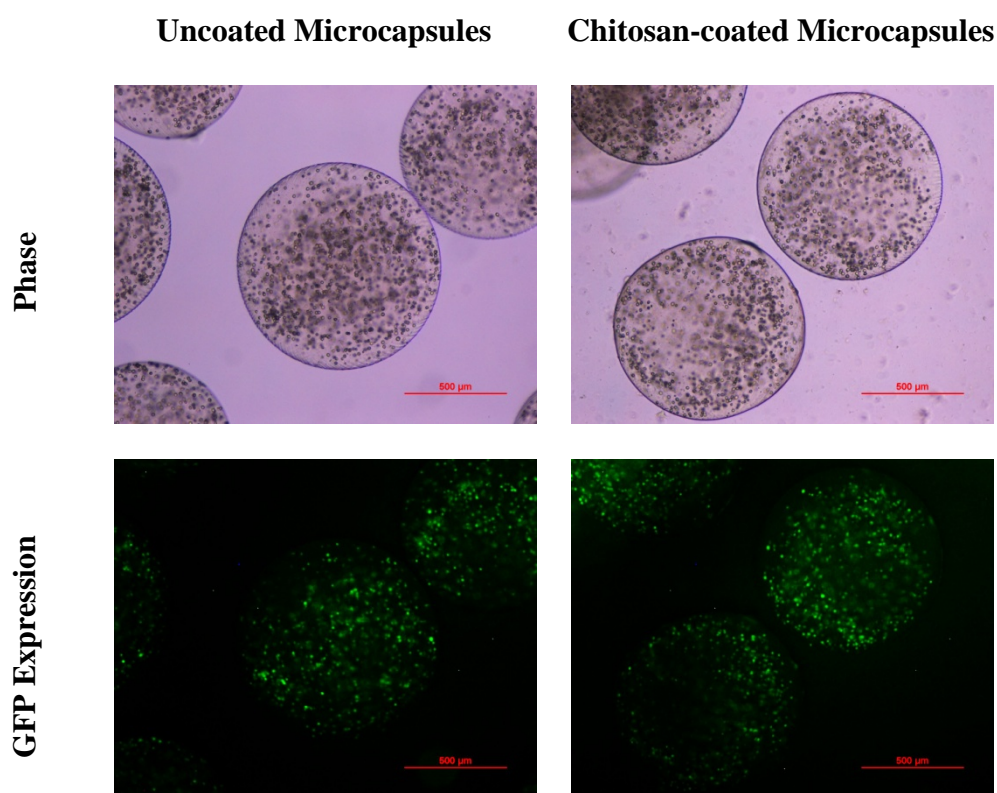


**Figure 3.13** Mouse OCT4-GFP embryonic stem cells are encapsulated in uncoated and chitosan-coated alginate microcapsules following fabrication. GFP expressions of encapsulated mouse OCT4-GFP embryonic stem cells are revealed using fluorescence microscopy. Microscopic images are taken at 4x magnification following microcapsule fabrication.

Following the encapsulation of mouse OCT4-GFP embryonic stem cells, the microcapsules are incubated in differentiation medium for 2 days at 37°C and 10% CO<sub>2</sub>

with medium change occurring every day. After 2 days, the proliferation and differentiation of the stem cells are analyzed using flow cytometry by means of fluorescence-activated cell sorting (FACS). The proliferation and differentiation of the encapsulated mouse OCT4-GFP embryonic stem cells is compared to the nonencapsulated state. Figure 3.14 provides the results from flow cytometry analysis.

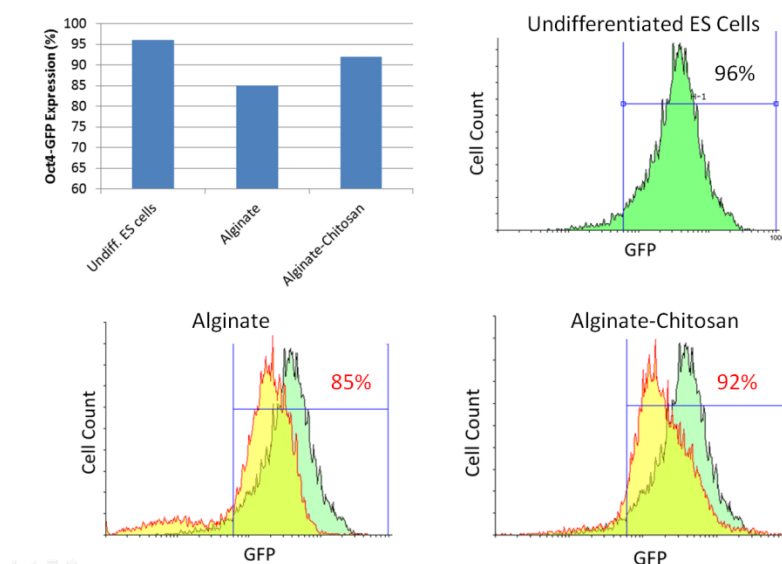


**Figure 3.14** Flow cytometry analysis of encapsulated mouse OCT4-GFP embryonic stem cells after 2 days of culture. The results reveal that the alginate microcapsule microenvironment can influence stem cell proliferation and differentiation.

Figure 3.14 shows that about 85% of the mouse embryonic stem cells expressed the OCT4-GFP gene when encapsulated in uncoated alginate microcapsules. On the other hand, about 92% of the stem cells expressed the OCT4-GFP gene when encapsulated in chitosan-coated alginate microcapsules. In summary, less OCT4-GFP expression means that more of the stem cells had differentiated. More expression of the OCT4-GFP gene reveals either slower differentiation or undifferentiation of mouse OCT4-GFP embryonic stem cells.

## CHAPTER 4

### DISCUSSION

The goal of this study is to optimize the physical properties of alginate-based microcapsules using a co-axial air flow method and examine how the 3D culture system of alginate microcapsules affects the proliferation and differentiation of mouse OCT4-GFP embryonic stem cells. Prior to the encapsulation of mouse OCT4-GFP embryonic stem cells, the necessary parameters for the alginate microcapsules are first determined. In biomedical applications, the microcapsules should have appropriate characteristics such as a round morphology, large pore sizes, and smooth surfaces in order to properly facilitate the bi-directional diffusion of the encapsulated material and surrounding environment. In addition, the microcapsule properties must be able to support cell physiological activities, such as metabolism, proliferation, migration, etc. for cell survival and function [3, 13, 14]. The selected materials for encapsulation fabrication should be compatible with the encapsulated material such that they do not disrupt its biological activity [2]. The microcapsules must also be mechanically stable and have long term integrity. These properties can be achieved by optimizing the size of the microcapsules to small dimensions. Small microcapsules are found to be mechanically stable due to the small diameter and large surface area to volume ratio [3, 6, 15]. It is important that microcapsules maintain the structural integrity and mechanical strength during its application [3].

In this study, microcapsules are produced by the extrusion of an alginate solution through a needle gauge with an application of an air flow. Microcapsule size can be

controlled by process parameters and liquid properties of the extrusion solution. The optimization of microcapsule size is investigated by varying the needle gauge size, air flow rate, and alginate concentration. The experiment of the effect of alginate concentration on microcapsule size is presented in Appendix. It is found that increasing the alginate concentration results in larger microcapsules. This is due to the increase in the viscosity of the alginate solution. Alginate solutions greater than 5% are difficult to prepare; and therefore is not generally used [9]. It is for this reason that the alginate concentration must remain below this value. The viscosity of the alginate solution not only affects microcapsule size, but also the shape of the spheres produced. The spheres become more spherical as the concentration of the alginate solution is increased. It is also known that the distance between the tip of the syringe needle and the gelation bath affects mainly the shape of the drops and thus the microcapsules. Munarin et al. found that the best results were obtained at a distance of 5cm [1].

Increasing the alginate solution concentration not only results in large microcapsules, but also in a decrease in microcapsule pore size; thus limiting diffusion [3]. Microcapsules larger than 1mm suffer from diffusion limitations that can result in reduced cell growth and cell death for encapsulated cells [16]. As mentioned previously, a microcapsule of small size with large pores is desired to efficiently facilitate diffusion. A higher membrane permeability offers a higher rate of nutrient exchange [16]. Therefore, an alginate concentration of low viscosity must be selected in order to produce small microcapsules with large pores. Based on the effect of alginate concentration on microcapsule size study, an alginate solution of 1.5% concentration is selected as the starting microcapsule material.

Not only must the microcapsules be small and have large pores, but they must also have a round morphology. Microcapsules are characterized for round morphologies by measuring their shape factor. The microcapsule can be associated to be a sphere if their shape factor is 1 or near 1; otherwise it is characterized to be an ellipse. The effect of needle gauge size and air flow rate on microcapsule size is studied. As it can be seen from Figure 3.1, microcapsule size decreases as needle gauge size and air flow rate both increase. Although the increase in air flow can result in smaller microcapsules, the number of microcapsules with round morphologies tends to decrease even though their shape factors are estimated to be 0.89. For example, microcapsules are produced by a 30 gauge needle with an alginate concentration of 1.5% and with air flow rates of 0, 7.5, 10, 15, and 20 SCFH. Air flow rates from 0 – 15 SCFH are able to produce round microcapsules, but anything higher than 15 SCFH, such as the 20 SCFH air flow rate, the round morphology of some of the capsules becomes distorted as shown in Figure 4.1. As a result, 15 SCFH is chosen as the air flow rate for the fabrication of alginate microcapsules in this study.

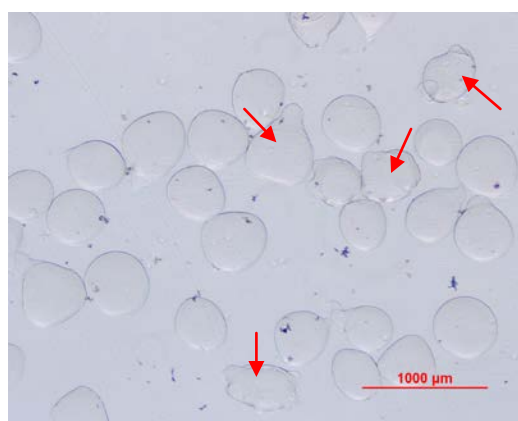


**Figure 4.1** Alginate microcapsules fabricated from 30 gauge needle, 1.5% alginate concentration, and 20 SCFH air flow rate result in irregular shaped spheres. Non-spherical shaped microcapsules are indicated by red arrows. Microcapsules are viewed under an inverted light microscope at 2x magnification.

It is important that the microcapsules maintain their structure and stability. Early rupture of the microcapsules would lead to the release of the entrapped drugs or cells before its intended application. The stability of the alginate microcapsules is further examined by adding an additional membrane coating, chitosan, on the surface of the sphere. Chitosan binds to the surface of the microcapsule thus creating a thin membrane with small pores. Chitosan is known to increase the stability of the alginate microcapsules and is able to minimize the loss of encapsulated material through ionic cross-linking with the carboxylic residues of sodium alginate. The electrostatic interaction between carboxylate groups of alginate and ammonium groups of chitosan leads to the formation of the chitosan-alginate polyelectrolyte complex [17]. Choosing the right chitosan concentration to coat the microcapsules is very important. If the chitosan concentration is too low, the stability of the microcapsules is not sufficient. However, if the chitosan concentration is too high, the permeability would be reduced due to the increase in chitosan-alginate complexes; therefore forming a stronger closer network [17]. A study conducted by Yu et al. demonstrated that 0.4% chitosan solution had the best reinforcement efficiency resulting in a slower release of the encapsulated substance [17]. Hence 0.4% chitosan solution is used in this work to coat the alginate microcapsules.

In this study, we examined the swelling behavior and stability of the alginate microcapsules. Both uncoated and chitosan-coated alginate microcapsules are incubated in PBS and monitored for two weeks. The results from the study reveal that uncoated alginate microcapsules swelled at a faster rate compared to the chitosan-coated alginate microcapsules. The explanation for the outcome could be that the alginate microcapsule

surface is directly exposed to the aqueous environment that it is placed in, which is in this case PBS. Alginate is highly hydrophilic due to the presence of  $-OH$  and  $-COOH$  groups in its chains. At neutral pH, water enters the chains of alginate and forms hydrogen bridges with the  $-OH$  and  $-COO^-$  groups. Consequently, the alginate egg-box model is slowly weakened and the alginate microcapsules swell. The swelling and rupture of alginate microcapsules is also due to the precipitation of calcium ions that would reverse alginate cross-linking when the spheres are incubated in PBS [3]. As there is a gradual decrease in the number of calcium alginate bonds, there is a decrease in gel strength and increase in permeability [1, 18, 19]. Adding an additional chitosan membrane on the alginate microcapsules can minimize the matrix swelling and increase stability. The chitosan-alginate polyelectrolyte complexes are difficult to break. The importance to monitor swelling behavior over time is to give an indication of the mechanical properties and durability of the microcapsules. The aqueous environment is one of the factors involved in the *in vivo* release kinetics of cells and drugs [1].

Next, the surface of the alginate microcapsules is characterized using FTIR, coomassie brilliant blue R-250 staining, and SEM. Each of these studies examine the absence or presence of chitosan on the surface of the alginate microcapsules. Alginate and chitosan powders are also scanned by FTIR for comparison with the FTIR spectra of uncoated and chitosan-coated alginate microcapsules. Recall that the gelation of alginate occurs when the carboxylate anions of guluronic acid crosslinks with the  $Ca^{2+}$  divalent cation. In addition, coating of the alginate microcapsules with chitosan occurs when the ammonium groups of chitosan crosslinks with the carboxylate groups of alginate thus forming the chitosan-alginate polyelectrolyte complex. FTIR analysis is able to detect

the structural modifications occurring in the polysaccharides during the formation of ionic crosslinks and polyelectrolyte complexes. The formation of crosslinks or polyelectrolyte complexes modifies the original structure of polysaccharides [1]. Therefore, the FTIR spectra of alginate and chitosan powders shift slightly in the FTIR spectra of uncoated and chitosan-coated alginate microcapsules though still remaining similar curves to their individual counterparts. The most important peak that indicates the presence of chitosan on the alginate microcapsule surface occurs at wavenumber  $1564\text{cm}^{-1}$ , which is not present on the uncoated alginate microcapsule spectrum.

The presence of chitosan on the alginate microcapsule surface is also detected through the staining of the microcapsules with coomassie dye brilliant blue R-250. The results presented in Figure 3.6 show that the chitosan-coated alginate microcapsules are stained well when compared to the staining of the uncoated microcapsules. The negatively charged coomassie brilliant blue R-250 would strongly bind to the positively charged chitosan polymer. The uncoated microcapsules are not stained well with the coomassie dye because the alginate polymer is also negatively charged. The binding of two negatively charged molecules is undesired. The structure of coomassie brilliant blue R-250 is illustrated in Figure 4.2.

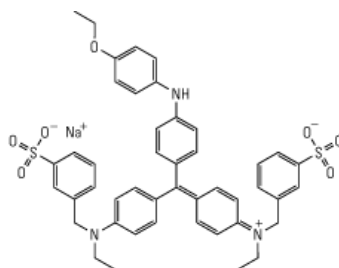


**Figure 4.2** The structure of coomassie brilliant blue R-250 consists of a negatively charged sulfate group.

Source: Syrový, L. and Hodný, Z. (1991). Staining and quantification of proteins separated by polyacrylamide gel electrophoresis. *J. Chromatog.* **569**, 175-196.

The surface topography of both uncoated and chitosan-coated alginate microcapsules are observed using SEM. The scanning electron micrographs of uncoated alginate microcapsules reveal a smooth surface. On the other hand, a few wrinkles, though not many, can be seen on chitosan-coated microcapsules. This could be due to the dehydration of the chitosan membrane surrounding the microcapsule [5]. In both conditions, the microcapsules are able to maintain their round morphology. Remember that round microcapsules with smooth surface are needed to aid in the diffusion of molecules into and out of the microcapsules.

Membrane permeability is an important characteristic of microcapsules for the encapsulation of cells. The permeability of the microcapsules is needed for the diffusion of oxygen and nutrients into the spheres in order to reach the encapsulated cells for growth and survival. In addition, diffusion of metabolic waste products and therapeutic molecules are needed to exit the microcapsules. Low molecular weight substances could be diffused out quickly and easily from the microcapsules leading to fast release and low encapsulation efficiency [17]. The permeability of the membrane is dependent on several properties such as charge distribution, porosity, hydrophilicity, and the properties and size of the substance being transferred across the membrane. These characteristics vary depending on the interaction of chitosan with alginate [20].

In this study, the permeability of the microcapsules is tested through the encapsulation and release of BSA and FITC-dextran. BSA is chosen for encapsulation because it is known to be an appropriate model protein in determining the permeability of microcapsules that are designed for biological systems. For the fabrication of the microcapsules, the alginate concentration is increased from 1.5% to 2.5% because it is

found that the microcapsules produced with 1.5% alginate following the mixing of the alginate solution with BSA and FITC-dextran resulted in tear drop shaped spheres. This is due to the dilution of the alginate solution once it is mixed with the encapsulated material. From the results of the BSA encapsulation study, a possible explanation for the significant amount of BSA released following fabrication and washing is the shape of the microcapsules produced. The microcapsules are not observed under an inverted light microscope for microsphere morphology. Microsphere morphology can greatly influence drug release behavior. Thus it is important to maintain the round morphology of the microcapsules. Another reason could be traced to the continuing formation of the ionic crosslinks and polyelectrolyte complexes of the microcapsules following fabrication. This would lead to the leakage of some of the encapsulated BSA out of the microcapsules.

Diffusion of the FITC-dextran molecules through the microcapsules is tracked by fluorescence microscopy. The results are presented in Figures 3.9 and 3.10. Based on the release studies of BSA and FITC-dextran, the microcapsules contain pore sizes large enough for nutrients in the cell culture medium to enter and reach to the encapsulated cells. Most differentiation agents, such as growth factors, typically have a lower molecular weight compared to the 70kDa FITC-dextran.

The microcapsule parameters reflecting cell viability and proliferation have to be defined for better application. The viability, proliferation, and metabolic activity of cells within the microcapsule can be influenced by factors such as the fabrication process, chemical and physical properties of the matrix material, microenvironments, etc. [3]. For example, recall that alginate solutions of high concentration result in larger size

microcapsules. The increase of microcapsule diameter would result in the reduction of cell viability. Alginate solutions with high concentration have higher surface tension, thus reducing the cell viability in the generated microcapsules [3]. In addition, nutrients and oxygen would not be able to reach the cells towards the center of the microcapsule as it would reach the cells on the outer ends in the microcapsule first. This would also result in a decrease in cell viability. The factors of the fabrication process that can also affect cell viability include air flow rate, stirring rate of the  $\text{CaCl}_2$  solution, and extrusion force (push speed). Effective evaluation of microencapsulated cell viability is highly important for better bioprocess control and quality assurance [4].

The viability of fibroblast cells encapsulated in alginate microcapsules, both uncoated and chitosan-coated, after the fabrication process is measured by a live-dead cell assay. Live-dead cell assay is a simple method involving the staining of cells with staining solution consisting of an aqueous solution, calcein-AM, and ethidium homodimer-1. Calcein-AM is a widely used green fluorescent cell marker that readily passes through the cell membrane and is retained in the cytoplasm of viable cells [11]. The live cells produce a green fluorescence at an excited wavelength of  $485 \pm 10\text{nm}$ . Dead cells are labeled with ethidium homodimer-1, emitting red fluorescence at  $530 \pm 12.5\text{nm}$  [4]. The results of the assay show that some cells are able to remain viable during the fabrication process of alginate microcapsules.

The viability of the cells in the microcapsules over time is evaluated through the biochemical assay, resazurin also known as alamar blue. Resazurin is a water-soluble extracellular redox indicator that can be reduced by living cells. Resazurin assay has its advantages of being nontoxic to cells and being directly proportional to the number of

viable cells [4]. The way in which the resazurin assay works is that the oxidized form of the alamar blue enters the cytosol and is converted to the reduced form by viable cells. The number of viable cells is related to the amount of the reduced form of alamar blue by evaluating the absorbance [1]. As presented in Figure 3.12, the number of viable encapsulated fibroblast cells decreases over time. More viable cells are detected in the uncoated alginate microcapsules compared to the fibroblast cells encapsulated in chitosan-coated alginate microcapsules. A possible rationalization for this could be that the resazurin solution could not easily diffuse into the microcapsules due to the additional chitosan membrane. Although this additional chitosan membrane provides stability for the microcapsules, it also reduces the size of the pores thus affecting the diffusion rate into and out of the spheres. Another reason could be traced back to human error. During the transfer and washing steps of the microcapsules and the aspiration of the solution in the wells each day, some of the microcapsules are lost during the process. Cell damage during the fabrication process may potentially be another explanation for the decrease in cell viability.

As a result from the two assays, a significant amount of the fibroblast cells remained viable initially as it is proved by the live-dead cell assay. However, they are unable to remain alive for a long period of time as it is shown by the results of the resazurin assay. The explanation can be linked to the fact that the cells are remained in suspension in the microcapsule despite the diffusion of the necessary nutrients to maintain cell viability and growth. It is necessary for cells to adhere to a surface in order to proliferate well.

Finally, the effect of the 3D microcapsule microenvironment on the proliferation and differentiation of mouse OCT4-GFP embryonic stem cells is studied. OCT4-GFP is a transcription factor protein with a green fluorescent protein that expresses a green fluorescence in undifferentiated embryonic stem cells. It is a frequently used marker for undifferentiated cells. Image of the nonencapsulated mouse OCT4-GFP embryonic stem cell subculture expressing the OCT4 gene is presented in Figure 4.3. The subculture is viewed under a fluorescence microscope at 10x magnification. Image is taken with a Nikon digital camera connected to the microscope.

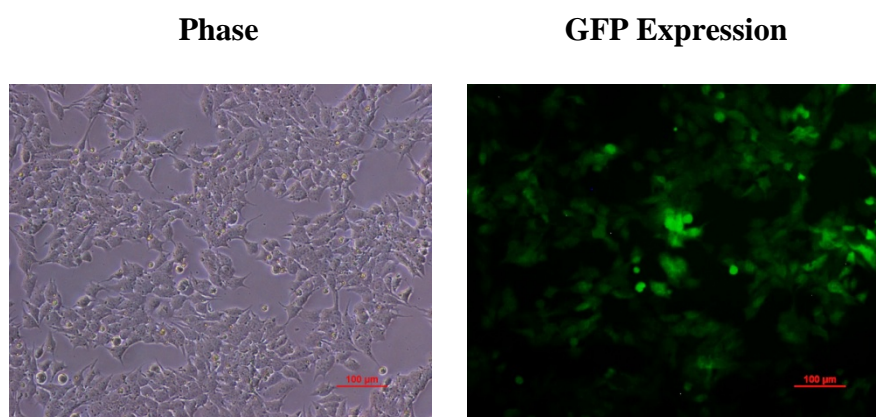


**Figure 4.3** Mouse embryonic stem cells expressing the OCT4-GFP gene by green fluorescence indicate that the cells are in an undifferentiated state.

After the encapsulation of mouse OCT4-GFP embryonic stem cells, the microcapsules are incubated in differentiation medium for two days with medium change occurring every day. On each day of culture, microcapsules are observed by fluorescence microscopy to detect any GFP expression of the cells within the spheres. After 2 days of culture, sodium citrate in sodium chloride is used to release the encapsulated mouse embryonic stem cells from the microcapsules. Sodium and citrate are non-gelling ions and chelators that can result in the dissolution of the alginate matrix. The cells are then

fixed with paraformaldehyde and analyzed using flow cytometry. Flow cytometry is used because the images by fluorescence microscopy alone are not sufficient enough to determine the success or failure of mouse embryonic stem cell differentiation. The results from flow cytometry analysis reveal that mouse embryonic stem cells are able to differentiate when encapsulated in alginate microcapsules. More differentiated stem cells are found with the uncoated microcapsules when compared to chitosan-coated microcapsules. Therefore, the 3D stem cell microenvironment has the ability to control the proliferation and differentiation of encapsulated mouse OCT4-GFP embryonic stem cells through microcapsule membrane coating.

## CHAPTER 5

### CONCLUSION

The main focus of this work is to optimize alginate-based microcapsules using a co-axial air flow method and study how the microcapsule microenvironment affects the proliferation and differentiation of mouse OCT4-GFP embryonic stem cells. The microcapsule parameters are first determined through a series of experiments that include the selection of microcapsule fabrication materials and optimization of microcapsule size. The microcapsules are then tested for mechanical stability and membrane permeability. Both of these characteristics are important for the application of these microcapsules in biomedical situations. The viability of cells within the microcapsules is then examined because it is crucial that cells remain alive prior to their purpose under study. Overall, the analysis from flow cytometry demonstrates that the microenvironment can control the proliferation and differentiation of mouse embryonic stem cells.

Some improvements may be necessary in the alginate microcapsule scaffold presented in this study. Future work can include finding ways to increase the cell viability within the microcapsules, coating the spheres with additional membranes to have a better control of the permeability, developing ways to produce uniform-shaped small spheres, and possibly try to differentiate the mouse embryonic stem cells to a specific lineage. Methods for mammalian cell encapsulation are constantly being improved to achieve smaller size microcapsules, better mechanical stability, lower shear exerted on the cell suspension during sphere formation, versatility in the selection of biomaterials, and higher throughput.

## APPENDIX

### EFFECT OF ALGINATE CONCENTRATION ON MICROCAPSULE SIZE

Figures A.1 and A.2 show the effect of alginate concentration on microcapsule size. Alginate concentrations of 1.5%, 2.0%, 2.5%, and 3.0% are tested. Each alginate solution is extruded through a 30 gauge needle with an application of 15SCFH air flow rate at the needle tip into 0.15M CaCl<sub>2</sub> solution under gentle stirring.

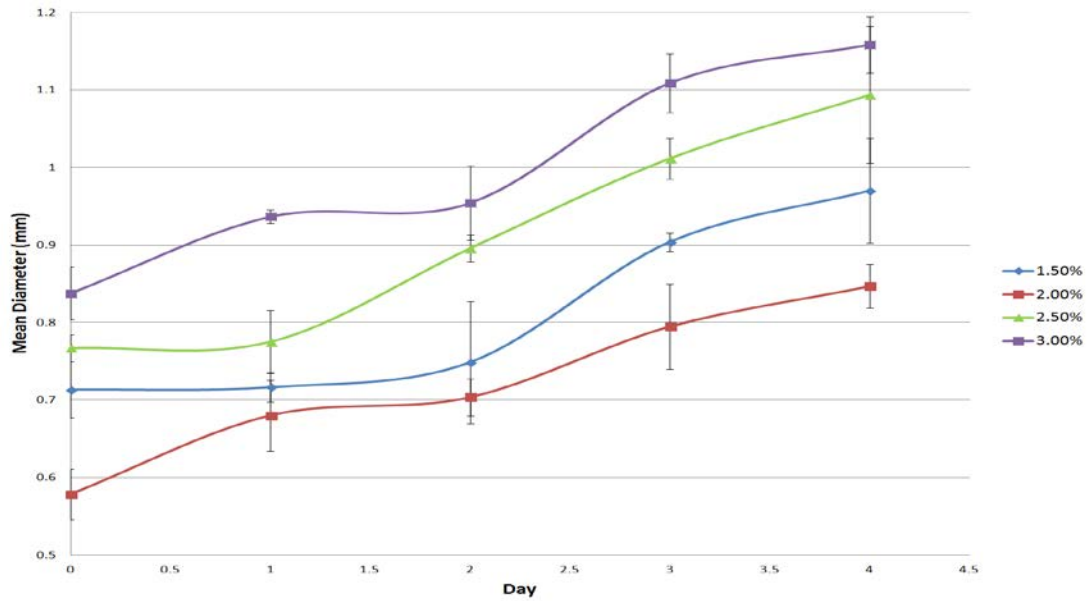


**Figure A.1** Increasing the alginate concentration results in larger size microcapsules. Alginate microcapsules are swelled and monitored for 4 days.

## REFERENCES

1. Munarin, F., et al., *Structural properties of polysaccharide-based microcapsules for soft tissue regeneration*. J Mater Sci Mater Med, 2010. **21**(1): p. 365-75.
2. Ma, Y., et al., *Microencapsulation of bacteriophage felix O1 into chitosan-alginate microspheres for oral delivery*. Appl Environ Microbiol, 2008. **74**(15): p. 4799-805.
3. Yao, R., et al., *Alginate and alginate/gelatin microspheres for human adipose-derived stem cell encapsulation and differentiation*. Biofabrication, 2012. **4**(2): p. 025007.
4. Xiao, J., et al., *Monitoring of cell viability and proliferation in hydrogel-encapsulated system by resazurin assay*. Appl Biochem Biotechnol, 2010. **162**(7): p. 1996-2007.
5. Yu, C.Y., et al., *Fabrication of microparticle protein delivery systems based on calcium alginate*. J Microencapsul, 2010. **27**(2): p. 171-7.
6. Hernandez, R.M., et al., *Microcapsules and microcarriers for in situ cell delivery*. Adv Drug Deliv Rev, 2010. **62**(7-8): p. 711-30.
7. Sakai, S., et al., *Biocompatibility of subsieve-size capsules versus conventional-size microcapsules*. J Biomed Mater Res A, 2006. **78**(2): p. 394-8.
8. Vandenberg, G.W., et al., *Factors affecting protein release from alginate-chitosan coacervate microcapsules during production and gastric/intestinal simulation*. J Control Release, 2001. **77**(3): p. 297-307.
9. Suksamran, T., et al., *Biodegradable alginate microparticles developed by electrohydrodynamic spraying techniques for oral delivery of protein*. J Microencapsul, 2009. **26**(7): p. 563-70.
10. Constantinidis, I., et al., *Non-invasive evaluation of alginate/poly-L-lysine/alginate microcapsules by magnetic resonance microscopy*. Biomaterials, 2007. **28**(15): p. 2438-45.
11. Zhang, W.J., et al., *Biocompatibility and membrane strength of C3H10T1/2 cell-loaded alginate-based microcapsules*. Cytotherapy, 2008. **10**(1): p. 90-7.
12. Dai, Y.N., et al., *Swelling characteristics and drug delivery properties of nifedipine-loaded pH sensitive alginate-chitosan hydrogel beads*. J Biomed Mater Res B Appl Biomater, 2008. **86**(2): p. 493-500.
13. Yang, S., et al., *The design of scaffolds for use in tissue engineering. Part I. Traditional factors*. Tissue Eng, 2001. **7**(6): p. 679-89.
14. Karageorgiou, V. and D. Kaplan, *Porosity of 3D biomaterial scaffolds and osteogenesis*. Biomaterials, 2005. **26**(27): p. 5474-91.
15. Uludag, H., P. De Vos, and P.A. Tresco, *Technology of mammalian cell encapsulation*. Adv Drug Deliv Rev, 2000. **42**(1-2): p. 29-64.
16. Breguet, V., et al., *CHO immobilization in alginate/poly-L-lysine microcapsules: an understanding of potential and limitations*. Cytotechnology, 2007. **53**(1-3): p. 81-93.
17. Yu, C.Y., et al., *Sustained release of antineoplastic drugs from chitosan-reinforced alginate microparticle drug delivery systems*. Int J Pharm, 2008. **357**(1-2): p. 15-21.

18. Kong, H.J., et al., *Controlling rigidity and degradation of alginate hydrogels via molecular weight distribution*. *Biomacromolecules*, 2004. **5**(5): p. 1720-7.
19. Shoichet, M.S., et al., *Stability of hydrogels used in cell encapsulation: An in vitro comparison of alginate and agarose*. *Biotechnol Bioeng*, 1996. **50**(4): p. 374-81.
20. Haque, T., et al., *In vitro study of alginate-chitosan microcapsules: an alternative to liver cell transplants for the treatment of liver failure*. *Biotechnol Lett*, 2005. **27**(5): p. 317-22.